MDPI

Review

Opportunities from Metal Organic Frameworks to Develop Porous Carbons Catalysts Involved in Fine Chemical Synthesis

Elena Pérez-Mayoral [1,*], Marina Godino-Ojer [2], Ines Matos [3,*] and Maria Bernardo [3]

[1] Departamento de Química Inorgánica y Química Técnica, Facultad de Ciencias, Universidad Nacional de Educación a Distancia, UNED, Urbanización Monte Rozas, Avda. Esparta s/n Ctra. de Las Rozas al Escorial Km 5, Las Rozas, 28232 Madrid, Spain

[2] Facultad de Ciencias Experimentales, Universidad Francisco de Vitoria, UFV, Ctra. Pozuelo-Majadahonda km 1.800, Pozuelo de Alarcón, 28223 Madrid, Spain

[3] LAQV/REQUIMTE, Departamento de Química, Faculdade de Ciências e Tecnologia, Universidade Nova de Lisboa, 2829-516 Caparica, Portugal

* Correspondence: eperez@ccia.uned.es (E.P.-M.); ines.matos@fct.unl.pt (I.M.)

Abstract: In the last decade, MOFs have been proposed as precursors of functional porous carbons with enhanced catalytic performances by comparison with other traditional carbonaceous catalysts. This area is rapidly growing mainly because of the great structural diversity of MOFs offering almost infinite possibilities. MOFs can be considered as ideal platforms to prepare porous carbons with highly dispersed metallic species or even single-metal atoms under strictly controlled thermal conditions. This review briefly summarizes synthetic strategies to prepare MOFs and MOF-derived porous carbons. The main focus relies on the application of the MOF-derived porous carbons to fine chemical synthesis. Among the most explored reactions, the oxidation and reduction reactions are highlighted, although some examples of coupling and multicomponent reactions are also presented. However, the application of this type of catalyst in the green synthesis of biologically active heterocyclic compounds through cascade reactions is still a challenge.

Keywords: metal organic frameworks; porous carbons; catalysis; fine chemicals

1. Introduction

As is well-known, MOFs are classified as crystalline porous coordination polymers in which poly-dentated organic ligands are coordinated to metallic centers [1,2]. Interestingly, a great variety of building blocks, comprising both metal centers and chelating ligands, can be used in MOF synthesis, resulting in high molecular and structural diversity. Among the characteristics of these materials are highlighted their low densities, large surface areas, and high pore volumes showing a permanent porosity, besides a controllable morphology. Advantageously, while the development of the porosity, both size and shape, in MOFs is a consequence of the assembly of both metal centers and organic ligands, the most-used inorganic porous materials often require the use of templates as structural-directing agents [3]. All these properties, together with the great structural variability of MOFs, make these materials highly versatile, with physico-chemical properties adapted for a specific application [4,5]. Nevertheless, metals as part of MOFs are uniformly and precisely distributed along their structures, often being the main active sites. In addition, other functional groups introduced into the MOF structure from either a carefully selected organic linker or by grafting (e.g., amines) by using the post-synthetic method [6] can be present.

In this context, the applicability of MOFs covers numerous application fields such as gas adsorption and separation, even much more than zeolites or activated carbons [7,8], energy storage and conversion [9], chemical sensing [10], organic pollutants degradation [11], heterogeneous catalysis [12], in particular in fine chemical production [13], and much more

recently in drug delivery [14], among others. Concerning the catalytic application of MOFs, the main disadvantage of these materials is their thermal stability, since often, the structure is collapsed at relatively low temperatures.

Considering both its high-developed porosity and that metals are perfectly located in MOF structures, these materials have been recently studied as emerging precursors of ordered porous carbons, in such a manner that the uniform porous network is maintained on the resulting carbon material [15]. In addition, some MOF-derived carbons, synthesized under strict and specific thermal conditions, show highly dispersed and abundant metal nanoparticles in high loadings, even at sub-nanometer level, pre-organized in a precursor MOF structure, at relatively low cost [16,17]. Summarizing, this area is in expansion as a new frontier, particularly in heterogeneous catalysis, since MOF-derived porous carbons present higher thermal stability than their precursors and enhanced porosity in terms of pore volumes and surface area, in addition to adjustable and uniform dopant distribution and, in some cases, the presence of metal phases atomically dispersed. All these characteristics, which directly influence the catalytic performance, are considered the main differences to the traditional porous carbons [18,19].

Based on the aforementioned, this review summarizes the main synthetic approaches to prepare porous carbon materials from MOFs, mainly focusing on their application in the clean synthesis of highly valuable compounds in the context of fine chemical synthesis. By selecting the appropriate MOF, even using other heteroatom sources, free-metal or heteroatom-doped porous carbons with highly developed porosity can be synthetized.

2. Porous Materials from Metal Organic Frameworks (MOF): Synthetic Strategies

The intention of the following paragraphs is to provide a small overview on the most common synthetic routes for the preparation of MOFs. This is a fast-growing topic of research and new materials and synthetic pathways are reported frequently. In the literature, there are already many reviews of MOFs for different applications where the different synthetic methods are described [20–23].

The nomenclature of these materials is also not straightforward, as sometimes it relates to its structure and/or components (e.g., ZIF—zeolite imidazolate framework), but often they are known by their place of finding (e.g., MIL—Materials Institute Lavoisier) [21,24].

As mentioned, MOFs are constituted by two main components: the metal ion and the organic ligands or linkers. The most commonly used metal ions are transition elements such as Cr^{3+}, Fe^{3+}, Co^{2+}, and Zn^{2+}, but MOFs with alkaline-earth metal ions and rare-earth metal ions can also be prepared [25]. The linkers are organic molecules with specific functional groups capable of coordinating to the metal, including carboxylic-acid-based linkers, nitrogen-containing heterocycles, phosphoryl and sulfonyl linkers, and cyano linkers, among others. A simple yet accurate description of the synthetic procedure for the preparation of these materials is the mixture of the two components, metal ions and linker, under mild conditions so that porous crystalline structures are obtained. Many methods have been described to obtain MOFs, such as the solvothermal method, mechanochemical method, microwave-assisted method, electrochemical method, sonochemical method, and layer-by-layer synthesis (Figure 1).

Figure 1. Schematic representation of MOFs synthesis.

Briefly, the solvothermal method consists of the mixture of the solutions of metal ions and the organic linkers in a specific solvent under chosen experimental conditions. These reactions are often carried out in autoclaves, at temperatures higher than the boiling point of the solvent in autogenerated pressure. Synthesis conditions are the determinants for the MOFs obtained, and the obtained structures and morphologies are controlled by parameters such as temperature, pressure, reagents composition, or type of solvent.

The mechanochemical method is when the mixture of the components is promoted by mechanical action in the absence of solvent. The metal salts and the organic linkers are ground together in a mortar, a ball mill, or other suitable equipment to promote the reaction. This is a simple and effective synthetic method; the reaction occurs through the mechanical breaking of the intermolecular bonds, and it takes place at room temperature. This method circumvents the use of solvents—a very significant advantage.

In the microwave-assisted method, the synthesis occurs under microwave radiation. This is a very effective way of heating because of the direct interaction of the radiation with the molecules in the reaction media. This method is used, aiming at rapid synthesis procedures but also to obtain nano-size crystals, to increase product purity and promote rapid crystallization.

The electrochemical method is considered to be a more environmentally friendly method as it does not use metal salts, thus avoiding the formation of corrosive and harmful anions [20,24]. Alternatively, the metal ion is introduced using an electrochemical process, such as the anodic dissolution method that uses an electrode as the source of metal ions. The electrochemical synthesis is also used in the production of thin films of MOFs over a surface.

To obtain MOF films, another of the techniques reported is layer-by-layer synthesis. The film is formed over a surface prepared for it by immersing the surface in solutions of organic ligands and metal ions sequentially. The orientation of the films seems to be dependent on the sequence used in the synthetic process, while the main parameters affecting growth are the metal source and the surface characteristics [26].

The sonochemical method is a synthesis procedure that employs ultrasound radiation (20 kHz–10 MHz), by which the acoustic cavitation phenomenon, with the formation, growth, and collapse of bubbles in solution, results in the formation of hotspots of very high local temperatures and pressures. Ultrasound does not react with the molecules, since it exceeds the vibrational wavelengths of atoms and molecules [27]. Applying the sono-chemical route, besides the reduction in reaction time, there is a homogeneous nucleation and the formation of significantly smaller particles, making this a possible and effective way to obtain nano-sized MOFs [28]. Experimentally, the solution mixture suitable to obtain the target MOF structure is introduced in a reactor fitted with a sonicator bar, allowing control over the power, and the correct parameters will result in fine crystallites of the desired MOF. A related method is designated by the soft spray technique [29] that consists of using ultrasonic vibration to obtain small drops of the solution that are then dispersed uniformly into another liquid or solid surface. This allows for uniform deposition and increased precision, thus increasing the possibility of controlling the micromorphology of the MOFs' architectures, as well as their chemical composition.

There are still other methods reported in the literature such as spray drying, ionic-liquid-assisted synthesis, and the diffusion method, among others. The selection of the synthesis method used is of great importance and determines the type and characteristics of the materials obtained, such as particle size distribution, porosity, and morphologies that have impact on the properties and application of the materials in adsorption, catalysis, sensors, etc.

It is also common to perform post-synthesis modifications of the MOF materials [20] to enhance or tune some specific characteristics directed at target application. Functionalization is one of the most often reported techniques to tune the properties of the material by introducing additional functional groups into the structure. Although this can be made directly via self-assembly during the synthesis process, it is often done via post-synthesis

methods. In the direct method, it is not always possible to introduce the desired functional group directly because the new linker may not be compatible with the reaction conditions or not able to produce the same MOF structure. On the other hand, the main challenge when doing post-synthesis modifications is to guarantee the integrity of the MOF structure throughout the process. For catalysis purposes it is frequently reported the incorporation of metal nanoparticles highly dispersed. The loading of metals is performed by incipient wetness method [30], by hydrothermal methods [31], or the precipitation method [32]. Another type of modification is the impregnation with active compounds, such as ionic liquids [33] or C48B12 molecules [23].

There are advantages and disadvantages to the different synthetic approaches. The solvothermal method, the more traditional one, has the advantage of being a one-pot method allowing single crystals at moderate temperatures; however, it has the disadvantages of high reaction times, the use of solvents, and easy formation of byproducts. The mecanochemical method, on the other hand, is a solvent-free method performed at ambient temperature, thus less hazardous; however, it can have problems of pore volume. The microwave-assisted method allows short reaction time and results in high-purity products with good control over the crystal size; however, some problems of reproducibility have been reported because of the use of different equipment, and the industrial scale of this methodology can be limited. The electrochemical method is an alternative that avoids the use of more hazardous solutions and can be operated in a continuous mode, allowing for higher production rates and facilitating possible industrial application; however, it requires specific conditions to work. The use of sonication for the synthesis has the advantage of being a fast and energy-efficient method, allowing the obtention of nano-sized crystals; nevertheless, there is no control over the local temperature of the reaction. [1,22] These and other aspects should be considered when selecting the most adequate synthetic method for a specific application.

2.1. MOFS from Waste

More recently, a new class of sustainable materials has emerged consisting of MOFs synthesized using components derived from waste. These developments are very interesting, not only in terms of environmental impact but also for the economical sustainability of the materials; therefore addressing the circular economy in the whole process [34,35]. This new concept of mining resources from waste is emerging as a solution for the sustainable scale-up of these materials, thus converting waste into MOFs is under increasing investigation [36,37].

Several approaches can be identified in the literature such as recovery of organic ligands from waste plastic through acid or basic hydrolysis, retrieval of metal salts from leaching solutions of metal containing wastes, or even insoluble metal precursors for heterogeneous synthetic routes [38].

From the depolymerization of polyethylene terephthalate (PET), terephthalic acid, which can be easily obtained, is one of the most-used organic ligands in MOF preparation, as is the case for the MIL synthesis. PET is one of the most commonly used plastics and has applications in short-lifetime products such as water bottles and food packaging; this makes this spent material an abundant resource, not always explored correctly. The chemical recycling of PET allows the production of the initial PET monomers, ethylene glycol (EG) and terephthalic acid (TPA), or other chemical products of interest. Starting from the plastic waste, chemical recycling may proceed via different processes, including glycolysis, hydrolysis, and methanolysis—hydrolysis being the most interesting one for MOF synthesis since it results directly in terephthalic acid [39]. In the last years, several reports can be found on the use of PET as the ligand source for the sustainable production of different MOFs [40–42]. Of particular interest is the possibility of producing the TPA (also known as H_2BDC) via PET hydrolysis and simultaneously form the MOF in a one-pot reaction, as reported by some authors [43,44]. Other waste plastics can be used as ligand sources, as in the case of polylactic acid as the lactic acid source for the synthesis of ZnBLD [45].

The other important component in MOF synthesis is the metal ion. The possibility of metal recovery from waste for the production of high-value-added materials such as MOFs has been the focus of some recent research. Electric and electronic waste (e-waste) and spent batteries are increasingly generated residues and can be considered good sources of recovered metals. The challenge is in recovering metal ion in high purity, which can be a tedious and costly process, thus impairing the feasibility of this valorization route for these wastes.

The synthesis of MOF-5 was reported using Zn^{2+} ions recovered from alkaline battery waste. Different procedures were tested to recover the zinc ion from the waste, and then the characteristics of the MOF prepared with the waste-derived metal were compared to an MOF prepared with pristine reagents, revealing high comparability between materials.

In another paper, using electroplating sludge (EPS) as a metal source, it was possible to synthesize chromium base MIL-53 via the hydrothermal method in a simple process [46].

More recently, the synthesis of MOFs using both components derived from waste was reported. Ni-MOF was prepared using PET as the source for the organic ligand (TPA) and using electroplating sludge as the metal source. The authors declared that even using the sludge directly, with other metal ions such as Fe^{3+}/Cu^{2+} ions coexisting with Ni^{2+} ions, could result in the successful fabrication of the MOF material [47].

2.2. Hierarchically Porous MOFs

Even though MOFs are known for their excellent properties, making the materials suitable for so many distinct applications, there are some drawbacks. MOFs are primarily microporous materials, meaning displaying pores sizes under 2 nm; this feature, although granting high surface areas and pore volumes, may hinder fast diffusion and mass transfer of the molecules because of the small pore aperture. This characteristic combined with the relatively large particle size may limit their applications related to larger molecules. Looking to overcome this issue, the development of hierarchically porous MOFs has been considered a successful approach [48]. In these new materials, larger pores are developed, and there is a combination of micro- and meso- or macro-pores in the structure [49–51]. To achieve the synthesis of hierarchical materials, there are different tactics; among them are the use of templates during the synthesis [51], solvent- or water-mediated synthesis [52,53], post-modification methods such as chemical-facilitated etching, etc.

Additionally, three types of hierarchy can be considered for MOF design: porous, architectural, and compositional hierarchies, as schematized in Figure 2. Porous hierarchy refers to different types of porosity within one framework. The architectural hierarchy allows the production of multicomponent architectures, while the compositional hierarchy allows the development of increasingly more sophisticated tailored structures.

2.3. Single-Atom Catalysts from MOFs

Single-atom catalysts (SACs) are a type of material presenting atomically dispersed active metal sites on the surfaces of solids. This feature is particularly relevant in the field of catalysis, and much effort has been devoted to this subject. The easiest way to obtain SACs is to immobilize the single active atoms directly in the surface of a support material. More recently, SACs based on MOFs have gained much attention because of the properties of the MOF but mostly because of the possibility of higher control over the design and tailoring of the catalytic properties, thus combining the advantages of SACs and MOFs with very positive results [21].

The single-metal sites in SACs based on MOFs can be created in the metal nodes and metallolinkers in the MOF framework during synthesis, or they can be introduced via functionalization of the MOF materials by coordination of the metal catalyst to the organic ligands or to unsaturated metal nodes, or by impregnation or incapsulating inside the pores. Several experimental methods have been reported to achieve this, including wet chemistry, atomic layer deposition, and pyrolysis [54,55].
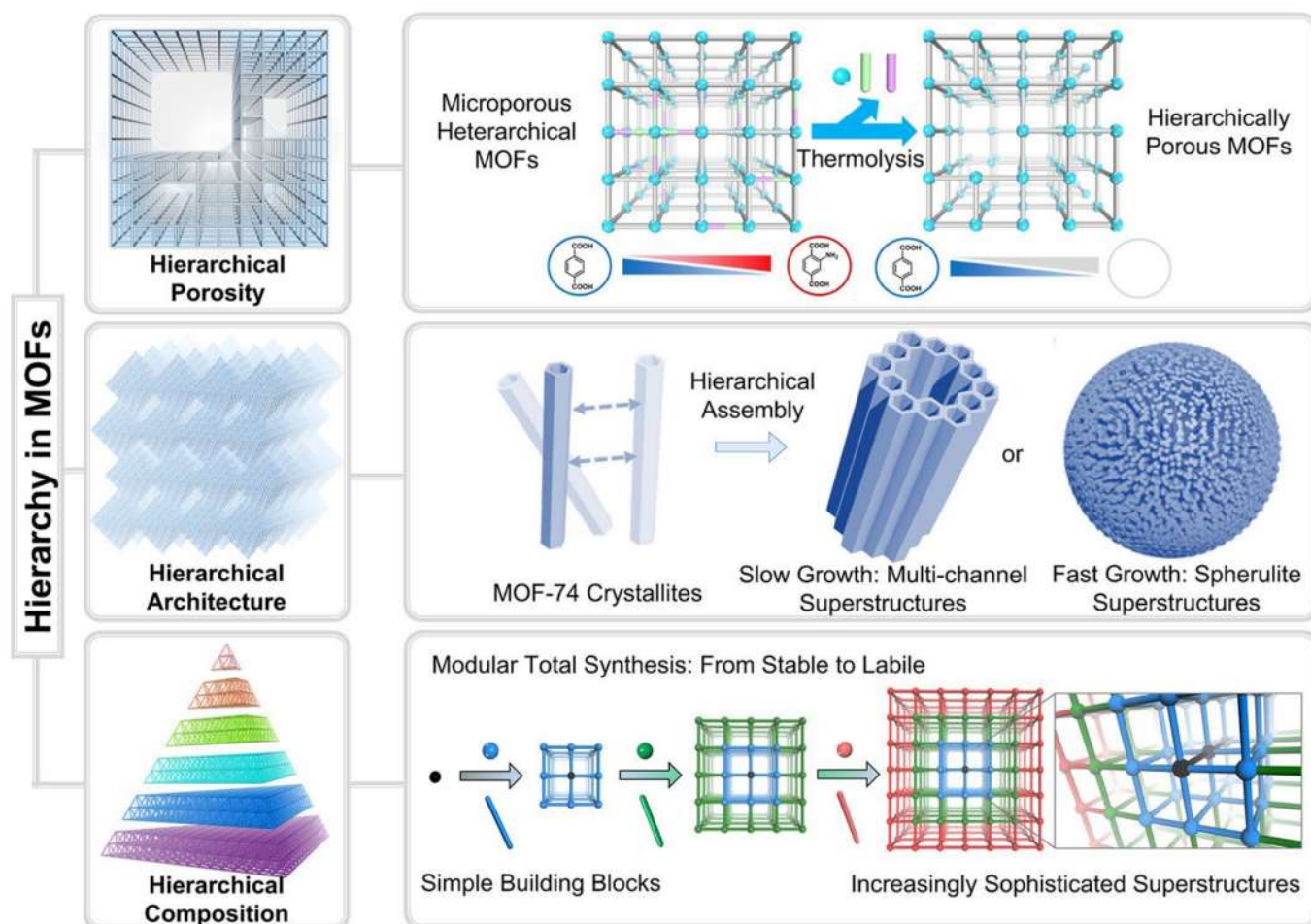
Figure 2. Hierarchically structured MOFs from three different perspectives: hierarchical porosity (top), hierarchical architecture (middle), and hierarchical composition (bottom). Reproduced with permission from ref. [48]. Copyright © 2020 American Chemical Society (further permission related to the material excerpted should be directed to the ACS).

Besides SACs based on MOFs, where the single metal is immobilized in the MOF framework, there are also other types of SAC materials that are MOF-derived SACs, including porous-carbon SACs; these will be detailed in the next section.

3. MOF-Derived Porous Carbons

The properties of porous carbons such as large surface area, tailored porosity, thermal and chemical stability, high electronic conductivity, and easy heteroatom doping, make them excellent catalysts and/or catalyst supports. Using MOFs as sacrificial templates/precursors of porous carbons has received great attention in the last years [56–59]. Submitting the MOFs to high temperatures under inert atmosphere (pyrolysis) generates carbons that might be impregnated with the metallic species (Zn, Co, Fe, Ni, Cu . . .) originally embedded on the MOF matrix and loaded with heteroatoms (O, N, S, P . . .) that composed the MOFs' organic ligands. Although direct pyrolysis of MOFs can promote a decrease in the original surface area, the resulting dispersion of metal and heteroatom active sites greatly improves the performance of the obtained carbons on catalytic reactions. Additionally, MOF-derived carbons possess higher stability to heat and water, overcoming these limitations of the pristine MOF [60].

The carbonaceous matrix of the porous carbons derived from MOFs results from the carbonization of the organic ligands of the MOFs' porous networks, and with a strict control

of the pyrolysis conditions, it is possible to tune surface properties. In addition, the original MOF structure and composition is crucial on the properties of the obtained carbons.

Direct carbonization of the MOF precursor has been the most-used technique to obtain MOF-derived porous carbons. Co-carbonization with additional carbon and heteroatoms sources has also been a common methodology. The post-treatment of the obtained carbons is applied for porosity enhancement and/or surface doping. The fabrication strategies along with the MOF itself allow the obtaining of the following classes of MOF-derived porous carbons: (i) pure and heteroatom-doped carbons; (ii) metal nanoparticle, metal oxides, or atomically dispersed metal-atom-containing carbons; and (iii) composites of the previous ones [61,62]. Figure 3 summarizes the different classes of MOF-derived carbons that can be obtained.
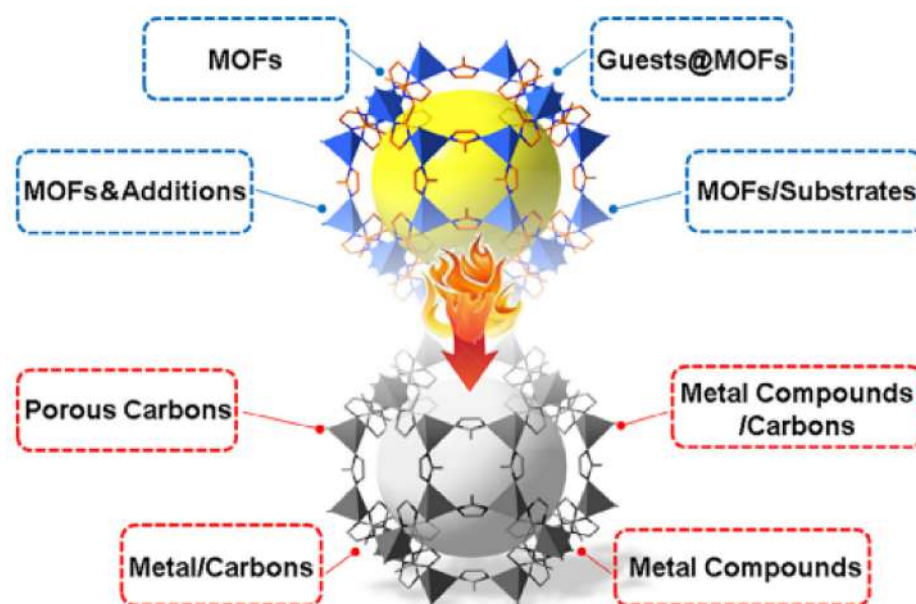

Figure 3. Classes of MOF-derived carbons. Reproduced from ref. [63]. Copyright © (2018) with permission from Elsevier.

Liu et al. [64] reported for the first time the use of MOF, namely MOF-5 (($Zn_4O(OOCC_6H_4COO)_3$), as a template for preparing porous carbons. In their work, the authors first polymerized furfuryl alcohol (PFA) inside the pores of MOF-5 and then carbonized the composite PFA/MOF-5 at 530 °C, 800 °C, and 1000 °C for 8 h under an argon flow (Figure 4). The carbon samples obtained at 530 °C and 800 °C presented much lower surface areas (217 mg^2/g and 417 m^2/g) than the sample obtained at 1000 °C (2872 m^2/g), since the ZnO that is formed in the carbonization is inside the pores. At temperatures above the boiling point of Zn (907 °C), the metal is evaporated, and the resulting metal-free porous carbon presented an increased porosity. For the samples produced at carbonization temperatures below the volatilization temperature of Zn, metal-free porous carbons were obtained from the HCl leaching of the metal that gives rise to an increase in the surface area from 217 to 1732 m^2/g.

Realizing that MOFs do not require an additional source of carbon because of the presence of organic ligands in their structures, studies about the direct carbonization of MOFs emerged [65–67], particularly about Zn-based MOF-derived carbons [61,68–72]. In fact, Zn-based MOFs have been preferably used as a template/precursor of metal-free porous carbons because of the easy removal of Zn either by vaporization or acidic solubilization. A particular case is ZIF-8 (Figure 5), which has been widely used to prepare porous carbons because it combines two important features: the easy sublimation of Zn and the imidazolate framework that provides an important source of nitrogen for *N*-doped carbons.

Figure 4. Schematic representation of porous carbons from MOF with furfuryl alcohol as an additional carbon source and direct carbonization of MOFs. Reproduced from ref. [65]. Copyright © (2013) with permission from the Royal Society of Chemistry.
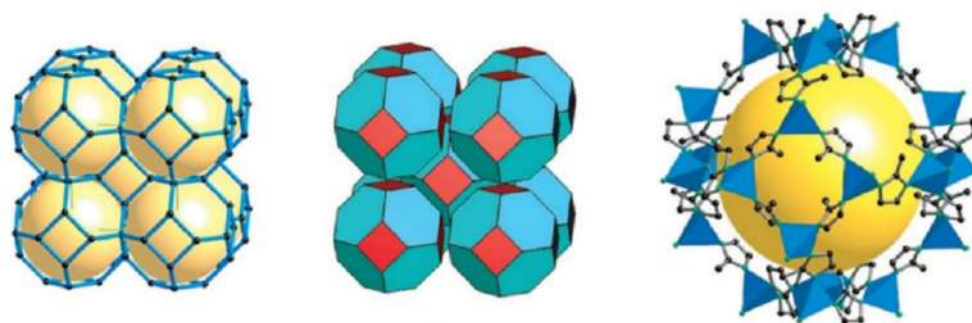

Figure 5. Crystal structure and simplified framework structures of ZIF-8 (Zn(2-methylimidazolate)₂). Reproduced with permission from ref. [73]. Copyright © 2006 National Academy of Sciences of the USA.

MOF-derived porous carbons with metal oxides, hydroxides, sulfides, phosphides, etc. can be intentionally produced during the pyrolysis of MOFs to exploit the features of the metallic species. In fact, MOF-derived porous carbons might constitute fine supports of SACs. The presence of N/S/O atoms from the MOF matrix provides anchoring sites for the single-metal atoms, avoiding the tendency of aggregation of the metal nanoparticles during the pyrolysis process [74]. However, the success of this strategy also depends on the choice of a proper MOF precursor (content of metal and heteroatoms) and on the pyrolysis conditions (pyrolysis temperature and time and atmosphere). Nitrogen-rich MOFs, such as ZIF MOFs, have been the most-used precursors to obtain strong *N*-metal bonds, granting thermal and chemical stability to the resultant materials with highly active centers for catalysis. If agglomeration of the metal nanoparticles cannot be avoided in the pyrolysis process, post-acid leaching allows the removal of the excess metal particles remaining in the atomically dispersed metal sites. Recent works have reviewed the strategies to obtain MOF-derived carbon-supported SACs [18,56].

Post-synthesis treatments in the obtained MOF-derived porous carbons can be employed, such as chemical activation with KOH that allows the obtaining of enlarged surface areas and exposes blocked active sites [19,57,75] (Figure 6). Acid leaching is applied when metal-free porous carbons are the target and pyrolysis temperature is not enough for metal sublimation.
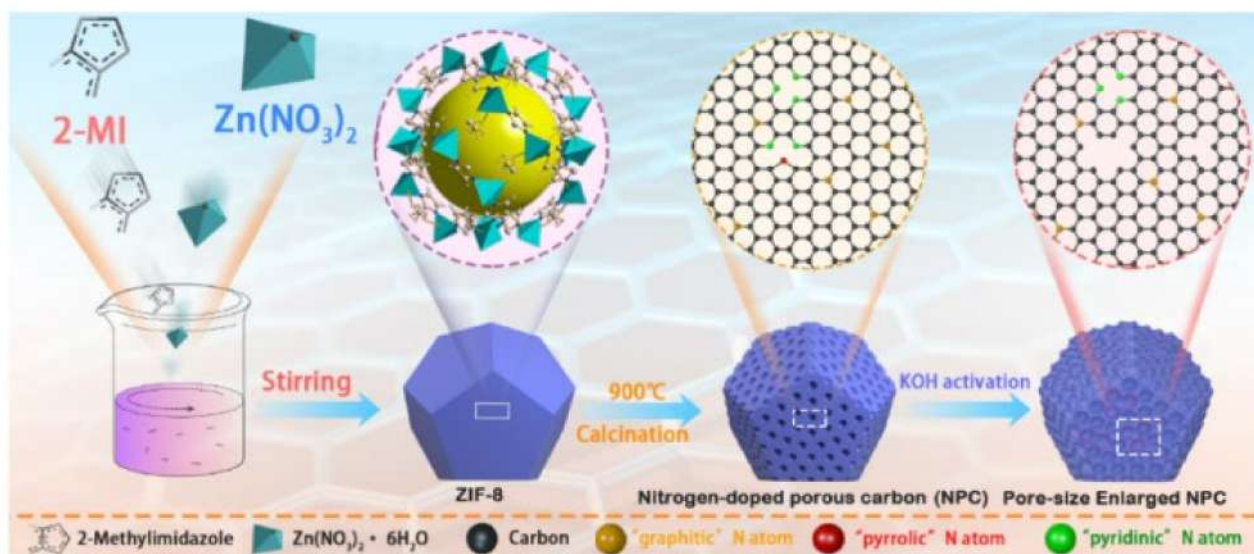
Figure 6. Synthesis of ZIF-8-derived porous carbon and KOH activation for pore enlargement. Reproduced with permission from ref. [75]. Copyright © 2019 American Chemical Society.

4. Catalytic Fine Chemical Syntheses by Porous Carbons from MOF

A variety of metal-porous materials, after careful pyrolysis of MOFs, can be produced, including metal oxides, carbides, nitrides, sulfides, and phosphides but also metal-free porous carbons, as mentioned above. Based on the topic of this review, this section is aimed at revising the different types of MOF-derived porous carbons applied to the catalytic synthesis of highly valuable compounds of interest, implying acid-base, oxidation–reduction and coupling catalyzed reactions of compounds with different functionalizations. In this context, the main investigated MOF structures to produce porous carbons are MOF-5, ZIF-8, ZIF-67, UiO-66-NH$_2$, and MIL-101-NH$_2$, among others.

4.1. Metal-Free Porous Carbons

In the last decades, metal-free carbons have attracted much attention as environmental-friendly catalysts in comparison to metal-based catalysts. In this context, synthesis of metal-free MOF-derived carbon catalysts is often achieved at high carbonization temperature under inert atmosphere, in some cases with metal species being removed by in situ evaporation or by subsequent acid treatment—Zn- or Co-based MOFs.

Although metal-based *N*-doped carbons from MOFs have been extensively studied in several oxidation reactions—e.g., hydrocarbons and amine oxidations and even epoxidation reactions—metal-free heteroatom-doped carbon catalysts have been also investigated in these transformations (Table 1).

Table 1. Metal-free MOF-derived porous carbon catalysts applied in fine chemical syntheses.

| Catalysts	Precursor	Catalytic Reaction	Ref.
N,P,S co-doped carbon	ZnCo-ZIFs@PZS	*Ethyl benzene to acetophenone* *Benzyl hydrocarbons to keto derivatives*	[76]
NPS-HCS	ZIF-67@PZS	*Aryl alkane oxidation*	[77]
B,N-PCs	Bio-MOF-1	*Reduction of 4-nitrophenol*	[78]
N-doped mesoporous carbons	ZIF-67 ZIF-8 Co-MOF-71	*Aerobic oxidation of cyclohexane, toluene to benzaldehyde and oxidative and coupling of benzylamine to N-benzylidene benzylamine*	[79]

PZS: poly(cyclotriphosphazene-co-4,4′-sulfonyldiphenol).

Such is the case of oxidation of ethylbenzene and related compounds catalyzed by N, P, and S co-doped hollow carbon shells synthetized from ZnCo-ZIFs@PZS composites (Scheme 1) [76]. The synthetic strategy consisted first of the synthesis of bimetallic ZIF-67 as a template under ultrasounds and treated with hexachlorocyclophosphazene and 4,4′-sulfonyldiphenol solution and triethylamine, used in different ratios, in such a manner that the former PZS is coating the MOF support [77]. Finally, the resulting composites were calcined at 900 °C under argon atmosphere and submitted to treatment with sulfuric acid and water. NPS-HCS showed a BET surface area of 1020 m^2 g^{-1} and a total pore volume of 1.21 cm^3 g^{-1} but also presented improved hydrophilicity mainly because of *N* doping. These catalysts exhibited good performance for selective oxidation of carbon–hydrogen bonds in ethyl benzene and related compounds in water at 80 °C in the presence of *tert*-butyl hydroperoxide (TBHP), yielding acetophenone with conversion up to 84% and selectivity ranging 92–99% higher than when using the related uncoated porous carbon (59% of conversion and 92% of selectivity). The authors concluded that the PZS coating procedure could be applied in the design of interesting heterogeneous catalysts. Note that the PZS-900-2h catalyst, obtained from PZS polymer by thermal treatment, promoted the reaction with notably lower conversion (12% after 6 h) and selectivity (66%). These catalysts resulted in also being active and selective for the oxidation of several benzyl hydrocarbons to the corresponding keto derivatives.
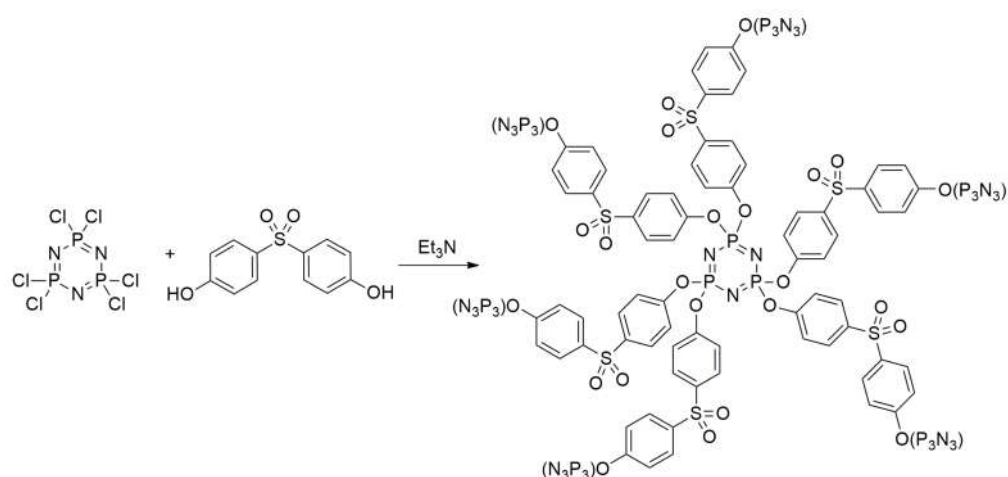

Scheme 1. Synthesis of the polymer poly(cyclotriphosphazene-co-4,4′-sulfonyldiphenol).

Interestingly, B–N co-doped porous carbon materials (BNPCs) from adenine-based bio-MOF-1 applied to the reduction in 4-nitrophenol have been also reported [78]. BNPC was prepared by pyrolysis of bio-MOF-1 at 1000 °C under N_2 atmosphere, obtained by coordination of Zn^{2+} with BPDC in the presence of adenine and washed with HCl. The resulting *N*-doped porous carbon, NPC, was treated with boric acid and submitted to thermal treatment at different temperatures, affording the mesoporous BNPCs a high degree of graphitization, in which N and B are homogeneously distributed (Scheme 2). BNPCs showed high catalytic performance and recycling stability in the reduction in 4-nitrophenol in the presence of $NaBH_4$ at room temperature. Conversion of 4-nitrophenol was influenced by the pyrolysis temperature, BNPC-1000 (1000 °C) exhibiting superior catalytic performance (95%) than the NPC sample. The authors proposed that a synergistic effect between dopants N and B in the porous carbon materials could be behind the catalytic activity.
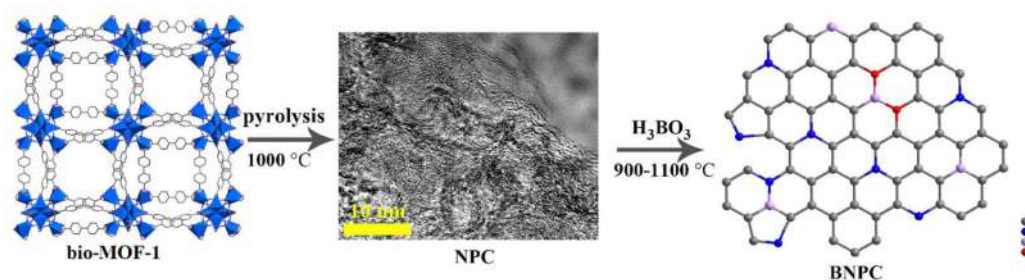
Scheme 2. Synthesis of nitrogen and boron co-doped porous carbon catalysts, BNPCs. Reproduced with permission from ref. [78]. Copyright © 2021 Elsevier.

Highly graphitized *N*-doped mesoporous carbons with high specific surface areas and large pore volumes and homogeneous distribution of dopant heteroatoms, obtained from direct pyrolysis of the corresponding MOFs—ZIF-67, ZIF-8, and Co-MOF-71—and subsequent treatment with aqua regia, were reported [79]. Porosity size is in situ created when removing the metal nanoparticles by acid etching and can be controlled by adjusting the carbonization temperature. These *N*-doped carbon materials were active in aerobic oxidation of cyclohexane at 125 °C, affording adipic acid in 15–48% of conversions and around 60% of selectivity. These results contrast with those obtained in the presence of a traditional Pd/C catalyst, in which selectivity is changed, leading to cyclohexanol/cyclohexanone as reaction products in 18% of conversions and 95 of selectivity. Oxidation of toluene to benzaldehyde was also possible with total selectivity even higher than when using the traditional Pd/C catalyst, although with low conversions. Finally, these catalysts can catalyze the oxidative coupling of benzylamine to *N*-benzylidene benzylamine in 99% of conversions, demonstrated by using structurally different amines, including substituted benzyl amines and even aliphatic ones (82–99%) (Scheme 3). The authors attributed the observed reactivity to the uniform distribution of nitrogen but also to the presence of accessible mesopores in samples.
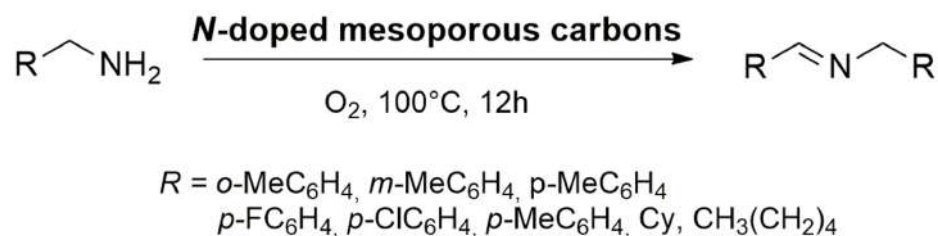
Scheme 3. Oxidative coupling of amines catalyzed by *N*-doped mesoporous carbons.

4.2. Metal-Doped Porous Carbons

Carbon-supported metal or metal oxide catalysts can be also prepared from MOFs by direct carbonization, under the appropriate thermal conditions, in such a manner that metal phases are embedded into a porous carbon matrix, as already mentioned. These metal-doped porous carbons have been applied in the synthesis of highly valuable compounds through oxidations, hydrogenations, coupling reactions, multicomponent synthesis of propargyl amines, and hydrodechlorination reactions (Table 2). Carbon materials doped with non-noble metals or metal oxides could constitute some of the most attractive alternatives to the high-cost noble metal catalysts.

Table 2. Metal MOF-derived porous carbon catalysts applied in fine chemical syntheses.

Catalyst	Precursor	Catalytic Reaction	Ref.
Oxidation reactions			
Cu@C	$Cu_3(btc)_2$	*Alcohol oxidation*	[80]
B-x (x = temperature)	MIL-88B	*Aryl or alkyl alcohol oxidation*	[81]
MDNM(75Zn25Mn or Ni)	(Zn/Mn or Zn/Ni) MOF-74s	*Benzyl alcohol oxidation and 4-nitrophenol reduction*	[82]
a-Cu@C	CuNbO-1 MOF: $([Cu(bpdc)(NO_2)_4)(H_2O)]_n$	*Benzyl alcohol to benzaldehyde*	[83]
Reduction reactions			
Cobalt-terephthalic acid MOF@C-800	Cobalt-terephthalic acid MOF-800	*Aryl, heterocyclic and aliphatic nitriles to amines Aryl, heterocyclic and aliphatic nitro compounds to amines*	[84]
Cu/Cu₂O/C	$Cu_3(btc)_2$/phenol formal-dehyde resin		[85]
Cu@C	$Cu_3(btc)_2$/H_3PO_4	*4-Nitrophenol reduction to 4-aminophenol*	[86]
Cu/Cu₂O@C	$Cu_3(btc)_2$ + GO		[59]
CuxO@C-400	$Cu_3(btc)_2$ +filter paper		[87]
a-Cu@C	CuNbO-1 MOF	*Nitrobenzene to aniline*	[83]
Ni/NiO@C	Ni-MOF-74	*Phenyl acetylene to ethyl benzene*	[88]
Ni@C/Ni-MOF-74	Ni-MOF-74	*Olefins hydrogenation to Alkanes*	[89]
M₂Si@C (M=Fe, Co, Ni)	MOFs-74/$Cl_2Si(CH_3)_2$	*Chemoselective hydrogenation of cinnamaldehyde*	[90]
Cu@C-H₂	$Cu_3(btc)_2$	*Butyl butyrate to buthanol*	[91]
Miscellaneous			
MOF-5-NPC-900-Pd	MOF-5 ($Zn_4O(H-bdc)_3$)	*Suzuki–Miyaura coupling reaction*	[92]
Cu/Cu₂O-rGO	MOFs-Cu_2O-rGO	*Sonogashira coupling reactions*	[93]
a-Cu@C	CuNbO-1 MOF	*Iodobenzene to N-aryl imidazole*	[83]
Cu@MOF-5-C.	$Zn_4O(bdc)_3$	*Multicomponent synthesis of propargyl amines*	[94]
Pd/MPC	Fe-MIL-88A	*Hydrodechlorination of 4-chlorophenol to phenol*	[95]
MOF-5-NPC-900-Pd	MOF-5 ($Zn_4O(H-bdc)_3$)	*Suzuki–Miyaura coupling reaction*	[92]
Cu@C	$Cu_3(bdc)_2$	*Azide–alkyne Huisgen cycloaddition reaction to obtain triazole*	[96]

bdc: 1,4-benzenedicarboxylate; **bpdc**: biphenyl 4,4′ dicarboxylic acid; **btc**: 1,3,5-benzenetricarboxylate.

4.2.1. Oxidation of Alcohols

$Cu_3(BTC)_2$ was used as precursor of a robust copper–carbon nanocomposite, Cu@C, by pyrolysis at 800 °C under argon atmosphere [80]. This material maintains the octahedron morphology of its counterpart and presents Cu^0 nanoparticles formed by reduction in Cu^{2+} ions in MOF during the thermal treatment. Cu@C assisted by 2,2,6,6-tetramethylpiperidine-*N*-oxyl (TEMPO) and *N*-methylimidazole (NMI) as a base showed an excellent catalytic performance in the aerobic oxidation of different alcohols affording the corresponding aldehydes in excellent yields. Interestingly, the oxygen content for the catalyst after recycling significantly increased, mainly because of the formation of CuO species during the oxidation reaction.

A similar synthetic strategy has been reported for the preparation of magnetic hybrid composites Fe_3O_4@C by pyrolyzing Fe-containing MIL-88B at different temperatures—500, 600, 700, or 800 °C [81]. Fe_3O_4@C hybrids showed a uniform distribution of Fe, C, and

O and, therefore, a high dispersion of Fe_3O_4 nanoparticles. A significant decreasing of the specific surface areas when increasing the pyrolysis temperature was observed, while Fe_3O_4 nanoparticles gradually formed aggregates and micropores present in precursor MOF totally disappeared in composites. Fe_3O_4@C composites were investigated in the green and selective aryl or alkyl alcohol oxidation, at 110 °C, in water, in the presence of H_2O_2, resulting in high catalytic performance and being selective to the corresponding keto derivative. The reaction took place in the absence of any base additives; the catalysts were magnetically separable and reused (four cycles) without almost any activity loss.

In the same context, Bhadra and Jhung [82] reported a mesoporous carbon doped with Ni or MnO nanoparticles, obtained from bimetallic MOF-74s (Zn/Ni or Zn/Mn using different ratios), highly reactive in the benzyl alcohol oxidation but also in the 4-nitrophenol reduction. In both cases, the best catalytic performance was reported when using the catalysts with the lowest Mn or Ni loadings, MDNM(75Zn25Mn or Ni), obtained by thermal treatment of the corresponding MOF-74 (75%Zn/25%Mn or Ni) precursor, even much more than in the presence of its homologous MnO/activated carbon, as demonstrated from the calculated TOF values (TOF = 1570, and 29 min^{-1} when using MDNM(75Zn25Mn) or MnO/activated carbon catalysts, respectively, for benzyl alcohol oxidation). The high reactivity was attributed to the high dispersion of the nanoparticles but also to the developed mesoporosity by Zn evaporation. Interestingly, the presence of Zn in the MOF precursors can serve to separate vicinal metal atoms, preventing the aggregation of the metal phase during the thermal treatment.

4.2.2. Hydrogenation Reactions

The development of clean methodologies for selective hydrogenation reactions is an important challenge for the scientific community. A few examples of MOF-derived porous carbons mainly containing Co, Ni, Fe, and Cu metallic phases have been reported for the hydrogenation reactions, such as hydrogenation of nitriles, nitro compounds, olefins, and even aldehydes and esters.

Hydrogenation of nitriles and nitro compounds: Nitroarenes and nitriles are important building blocks involved in amine synthesis as relevant intermediate compounds of capital importance. In this context, several porous carbon catalysts have been reported. Murugesan et al. [84] developed a reusable carbon-based catalyst constituted by graphene-shell-encapsulated Co_3O_4/Co particles (cobalt-terephthalic acid MOF@C-800) that are highly active and selective for the hydrogenation of structurally different benzonitriles to the corresponding benzyl amines, in the presence of H_2 or NH_3, in good to excellent yields (85–95%). This methodology also tolerates a great variety of functional groups such as esters, amides, and even C–C double and triple bonds and halogens. This catalyst was also able to catalyze the reduction in several structurally different molecules containing the nitro group to the corresponding amines, obtained in gram scale. The followed strategy was to synthesize the corresponding MOF in the presence of additional carbon as a powder and after that to pyrolyze the mixture at 800 °C, resulting in the most active catalyst. Remarkably, the unpyrolyzed MOF–carbon (cobalt-terephthalic acid MOF@C) but also the cobalt-terephthalic acid MOF were almost inactive for the investigated transformation, probably because the cobalt-terephthalic acid MOF@C-800 catalysts presented both types of nanoparticles, Co_3O_4 and Co^0; this last as a small-size particle in low quantity.

Several examples of MOF-derived porous carbons have also been reported for the hydrogenation of nitro compounds. Among the highly polluting compounds, 4-nitrophenol is widely used for industrial applications—textile, printing, pharmaceutical industries, and petrochemicals—originating water waste [18]. Among the most-used MOF precursors, $Cu_3(BTC)_2$ is highlighted, which converted into the corresponding porous carbons using different synthetic approaches that have been investigated in the 4-nitrophenol reduction to 4-aminophenol, in the presence of $NaBH_4$ and in water at room temperature (Table 2) [59,85–87].

Hydrogenation of C=C and C=O bonds: Guo et al. [88] reported mesoporous Ni/NiO@C core-shell nano catalysts showing zero-valent Ni nanoparticles from Ni-MOF-74 by pyrolysis at 500 °C under argon atmosphere. Ni/C presented an excellent catalytic performance for the hydrogenation of phenylacetylene to ethyl benzene (97%), in ethanol, at 50 °C, under H_2 atmosphere. In the same context, Nakatsuka et al. [89] reported on the synthesis of Ni-based catalysts (Ni@C/Ni-MOF-74), by thermal treatment at low temperature (300 °C) of Ni-MOF-74, in which Ni^{2+} nanoparticles are reduced to Ni^0 metal, highly active in the hydrogenation of olefins in ethanol, at 30 °C under reductive atmosphere (H_2, 1 atm). Catalytic performance of Ni-MOF-74-300 was superior to those observed for the Ni-MOF-74 precursor or even to NiO-supported activated carbon (Ni/AC-300). The authors highlighted that the Ni thermal decomposition on Ni-MOF-74 is different than in the case of Ni/AC-300, in which the Ni nanoparticles are oxidized by oxygenated functions in abundance at the carbon surface. Remarkably, a structural change in a sample carbonized at 300 °C, Ni-MOF-74-300, was observed developing mesopores, whereas a microporous structure derived from Ni-MOF-74 was maintained.

Interestingly, Zhang et al. [90] reported a series of nanocatalysts composed by transition metal silicides highly dispersed on porous carbon ($M_2Si@C$ (M=Fe, Co, Ni)) active in the hydrogenation of cinnamaldehyde. The synthetic approach consisted of microwave-assisted silicification of porous carbon-matrix-encapsulated transition metal (M@C) from MOFs-74 with dimethyldichlorosilane ($Cl_2Si(CH_3)_2$). Upon microwave irradiation, $Cl_2Si(CH_3)_2$ decomposed at the surface of metal nanoparticles, producing silane (SiH_4), which is able to react with metal nanoparticles leading to metal silicides. Activity of $M_2Si@C$ (M=Fe, Co, Ni) was superior in comparison with M@C counterparts probably because the carbon layers over metal nanoparticles are destroyed during the surface modification originating more active catalytic sites. It is noteworthy that $Ni_2Si@C$ resulted in higher activity than that for $Co_2Si@C$ or $Fe_2Si@C$ in the chemoselective cinnamaldehyde hydrogenation. While $Co_2Si@C$ catalyst was mainly involved in the hydrogenation of the C=O bond in cinnamaldehyde, selectivity to cinnamyl alcohol ranging 60%, a $Ni_2Si@C$ sample resulted in being highly chemoselective for the hydrogenation of C=C bonds, selectively affording hydrocinnamaldehyde (90%). These results strongly suggested different reaction pathways as a function of the reactant adsorption on the catalyst surface depending on the polarization properties of MSi intermetallic compounds.

The hydrogenation reaction of esters catalyzed by MOF-derived porous carbons has also been reported. At this regard, Zhao et at. [91] developed an MOF-derived core-shell Cu@C by direct pyrolysis (350 °C) of $Cu_3(BTC)_2$, an MOF widely investigated in fine chemical synthesis, under H_2 or N_2 atmosphere. Cu@C presented highly dispersed encapsulated Cu^+/Cu^0 species on a carbon surface, both copper species acting in cooperation in the hydrogenation of butyl butyrate, activating both reagents, butyl butyrate and H_2. While Cu^+ activated the ester, Cu^0 worked in the H_2 decomposition. Cu@C-H_2 was found to be the most active catalyst leading to butanol in 97% of conversions and 100% of selectivity. The authors compared the catalytic performance of Cu@C-H_2 and Cu@C-N_2 with those for conventional Cu-supported activated carbons, Cu/AC-N_2 and Cu/AC-H_2 prepared by using the impregnation method. Taking into account that the Cu/AC-N_2 sample barely catalyzed the reaction (1% of conversion vs. 17% for Cu@C-N_2), it was possible to conclude that the Cu^0 and Cu_2O phases are the truly catalytic-active species. Similar enhancement of conversion values was observed for the Cu/AC-H_2 (14%) and Cu@C-H_2 (27%) samples, demonstrating the superior catalytic performance of MOF-derived porous carbons. In addition, Cu@C-N_2 was submitted to reduced treatment in the presence of H_2, higher conversion, although lower than that observed for Cu@C-H_2, being obtained. Both the higher dispersion and adequate Cu^+/Cu^0 ratio should be then behind the observed catalytic performance.

4.2.3. Coupling Reactions

MOF-5 (Zn$_4$O(H-BDC)$_3$ has also been studied as a precursor of porous carbons in which Pd nanoparticles were immobilized [92]. The synthetic approach comprised (i) the direct pyrolysis of MOF-5 at different temperatures (700–900 °C), (ii) impregnation with H$_2$PdCl$_4$ and subsequent reduction with NaBH$_4$, and finally, (iii) thermal treatment at 900 °C. Zn-free MOF-5-NPC-900-Pd was also synthetized after acid treatment with HCl. In this case, the optimal carbonization temperature was 900 °C, leading to a microporous MOF-5-NPC-900 sample also containing some macropores and exhibiting high surface area (2478 m^2 g^{-1}). The BET area significantly increased after acidic treatment but also diminished after Pd impregnation because of the presence of well-dispersed Pd^0 nanoparticles installed in the hollows of Zn-free MOF-5-NPC-900. Catalytic performance was investigated in the Suzuki–Miyaura coupling reaction between differently substituted phenyl boronic acids and aryl bromides, in the presence of mixtures of EtOH-H$_2$O at 25 °C, Zn-free MOF-5-NPC-900-Pd affording the highest yield to the corresponding substituted biphenyls. Textural parameters, nanoparticles dispersion, and accessibility of active sites were behind the catalytic activity.

Sun et al. [93] developed an easy and efficient synthetic methodology to prepare Cu/Cu$_2$O-rGO, in which reduced graphene presents homogeneously dispersed Cu^0 and Cu$_2$O nanoparticles, able to efficiently catalyze the Sonogashira cross-coupling reactions. Cu/Cu$_2$O-rGO catalyst was prepared through a novel MOF jacket-structure, with "take" and "off" steps followed by an in situ reduction process (Scheme 4). The catalyst was tested in coupling reaction between phenylacetylene and aryl iodide, in the presence of Cs$_2$CO$_3$, in dimethyl formamide (DMF) at 80 °C, affording 1,2-diphenylethyne in excellent yield (91%), notably higher than when using Cu$_2$O-rGO or Cu-rGO as catalysts with a single Cu phase, then demonstrating a synergistic effect between both phases.
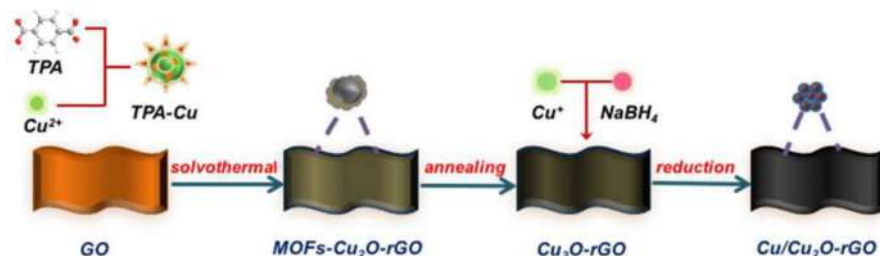
Scheme 4. Synthetic approach for the preparation of Cu/Cu$_2$O-rGO catalyst. Reproduced with permission from ref. [93]. Copyright © 2003 Royal Society of Chemistry.

Interestingly, Nguyen-Sorenson et al. [83] reported a novel and robust porous carbon catalyst, a-Cu@C, which presented an unusual morphology as layers of an anisotropic carbon structure. a-Cu@C catalyst was obtained by thermal decomposition of CuNbO-1 MOF ([Cu(BPDC)(NO$_2$)$_4$)(H$_2$O)]$_n$ and successfully applied to the *N*-arylation of imidazole in DMSO, in the presence of KOH at 110 °C (Scheme 5). The authors highlighted that CuNbO-1 decomposes at a notable lower temperature than other Cu-based MOFs such as Cu$_3$(BTC)$_2$, allowing the high dispersion of the copper species, as a mixture of oxidation states at the carbon surface, and then avoiding the sintering that often occurs at higher temperatures. a-Cu@C resulted also in being active for benzyl alcohol oxidation and nitrobenzene reduction.
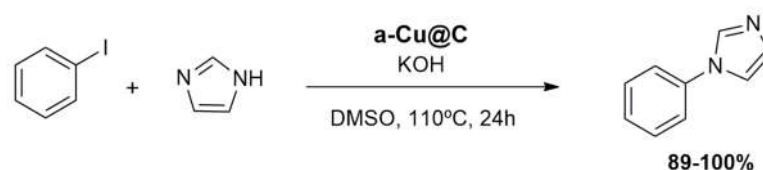
Scheme 5. *N*-arylation of imidazole catalyzed by a-Cu@C.

4.2.4. Synthesis of Propargylamines

Multicomponent reactions are one-pot processes that selectively lead to a unique reaction product, through cascade reactions, widely used in the synthesis of compound libraries. In this context, propargylamines are relevant compounds to produce heterocycles and, therefore, of great importance for pharmaceutical companies. MOF-derived carbons have also been reported for the synthesis of this type of compound. Concretely, MOF-5-C was prepared by pyrolysis of MOF-5 ($Zn_4O(BDC)_3$) and used as support of copper nanoparticles by using the conventional impregnation method [94]. It was found that Zn, ZnO, Cu, and CuO are present in Cu@MOF-5-C, resulting in highly porous carbon with a hierarchical pore structure, high in both surface area (2039 m^2 g^{-1}) and total pore volume (1.86 cm^3 g^{-1}). Cu@MOF-5-C was successfully applied in the multicomponent synthesis of propargyl amines from aldehydes, alkynes, and amines in toluene at 110 °C, exhibiting high catalytic activity (Scheme 6).
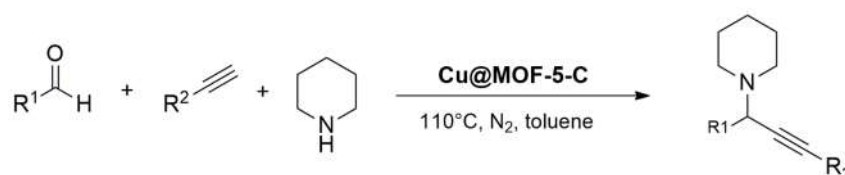

Scheme 6. Synthesis of propargyl amines from aldehydes, alkynes, and amines in toluene at 110 °C catalyzed by Cu@MOF-5-C.

4.2.5. Hydrodechlorination Reactions

Dong et al. [95] reported the pyrolysis (700 °C) of Fe-MIL-88A affording a magnetic metal mesoporous carbon (MPC), in which γ-Fe_2O_3 and Fe_3C are the major metallic species. MPC was used as support of highly dispersed Pd nanoparticles; Pd/MPC was prepared by using the impregnation–reduction method. Pd/MPC as mesoporous carbon material exhibiting high surface area resulted in high catalytic activity (up to 90% of yield after 60 min) and reusability in the green hydrodechlorination of 4-chlorophenol to phenol in water at 25 °C, in the presence of NaOH as a neutralizing agent of released HCl, compared to other reported catalytic systems, such as Pd–Al pillared clays, prepared by either the impregnation method or by ion exchange, and even a novel fibrous nano-silica (KCC-1)-based nanocatalyst (Ni@Pd/KCC-1). Its high activity was mainly due to the high dispersion and accessibility of Pd nanoparticles. Pd/MPC was also highly active in the reduction in 4-nitrophenol.

4.2.6. Cycloaddition Reactions

Interestingly, $Cu_3(BTC)_2$ was successfully used upon both high pressure and temperature (400 °C) to develop a copper–carbon composite (Cu@C) containing fine copper nanoparticles [96]. Remarkably, Cu nanoparticles in Cu@C-400, mainly composed by Cu^0 partially oxidized at the surface, presented a smaller size than those when pyrolyzing $Cu_3(BTC)_2$ under atmospheric pressure, then avoiding sintering processes. Cu@C was applied to the azide–alkyne Huisgen cycloaddition reaction between benzylazide and phenylacetylene, in 1,4-dioxane as solvent and triethylamine as base, yielding the corresponding triazole in 28–16% after 1 h of reaction time (Scheme 7).
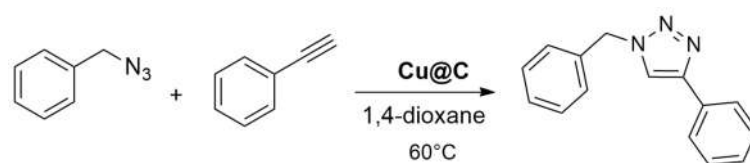
Scheme 7. Azide–alkyne Huisgen cycloaddition reaction between benzylazide and phenylacetylene catalyzed by Cu@C.

4.3. N-Doped Porous Carbons

Development of heteroatoms (*N*, *B*, *P* or *S*)-doped porous carbons is one of the strategies to modulate the intrinsic properties of carbon materials, allowing improvement of their catalytic performance. Particularly, N doping produces the formation of defects into the porous carbon structure because of the superior electronegativity of N regarding the vicinal C, in addition to the presence of new electron states, which can enhance the interaction capacity with other molecules. Furthermore, N can stabilize the presence of atomically dispersed metals at the carbon surface. In this context, the main MOF types to produce *N*-doped porous carbons are zeolitic imidazolate frameworks (ZIF) but also others containing nitrogen organic linkers, although it can also be synthetized by using additional nitrogen sources, as mentioned in the sections above.

A great variety of metallic *N*-doped porous carbons from MOFs applied in the synthesis of valuable compounds through oxidation and reduction reactions but also in coupling, cycloadditions, and acid-base catalyzed reactions have been reported (Table 3).

Table 3. Metal *N*-doped MOF-derived porous carbon catalysts applied in fine chemical syntheses.

Catalyst	Precursor	Catalytic Reaction	Ref.
Oxidation reactions			
Co/C–N	$Co_9(btc)_6(tpt)_2(H_2O)_{15}$	*1-phenylethanol to acetophenone*	[97]
Co@C−N	Zn/Co-ZIF	*Benzylic alcohols to ketones*	[98]
Ru3/CN	Ru3(CO)12@ ZIF-8 MOF	*2-aminobenzyl alcohol to 2-aminobenzaldehyde*	[99]
Ni@C-N	Ni-bdc-dabco-based MOF	*Alkane derivatives to ketones*	[100]
Pd–Cu@HO-NPC	HKUST-@ImIP	*Hydrocarbons to ketones*	[101]
C-N-Co (ZC-700)	ZIF-67	*Epoxidation reactions of olefins*	[102]
Co-CoO@C-N	Zn/Co-ZIF		[103]
Co-CoO@Ndoped	Cobalt MOF (ZIF-67)	*Alcohols to esters*	[104]
C-N-Co	ZIF-67	*p-nitrobenzyl alcohol to methyl p-nitrobenzoate*	[105]
Reduction reactions			
Co@CN	$[Co(tpa)(dabco)_{0.5}]$	*Cinnamaldehyde to cinnamal alcohol*	[106]
Co@Pd/NC	ZIF-67	*Nitrobenzene to aniline*	[107]
Co-CoO@N-C 25	ZIF-67	*Nitrobenzene to aniline*	[108]
$Zn_{0.3}Co_{2.7}@NC$	$Zn_{0.3}Co_{2.7}$-ZIF	*4-Nitrophenol to 4-aminophenol*	[109]
Table 1 (continuation)			
$Cu/Cu_xO@CN$	$Cu_2(bdc)_2(bpy)$	*4-Nitrophenol to 4-aminophenol*	[110]
$Ag_1Pd_9@NPC$-UiO-66-800	NH_2-UiO-66	*Nitrobenzene to aniline*	[111]
Co/N@C-800	ZIF-67@PVP	*Nitrobenzene to aniline*	[112]
Co@CN	$[Co(tpa)(dabco)_{0.5}]$	*Cinnamaldehyde to cinnamal alcohol*	[106]
Pd/NPC-ZIF-8	ZIF-8	*Vanillin to vanillin alcohol an p-creosol*	[113]
Co@C-N	$Co(bdc)(ted)_{0.5}$	*Transfer hydrogenation reactions*	[114]
Co-Ni(3:1)@C-N	(M-M'(1,4-bdc)$_2$(dabco)]·4DMF· 1/2H$_2$O,M/M'=Co,Ni,Cu)	*N-benzylidenebenzylamine via benzonitrile*	[115]
$CoNi@NC_x$	ZIF-67	*Hydrosilylation of cyclohexanone*	[116]
Pd-MDPC	ZIF-67	*Alkynes to olefins*	[117]

Table 3. *Cont.*

Catalyst	Precursor	Catalytic Reaction	Ref.
Pd@CN	ZIF-67 ((DICY; PVP)	*Hydrogenation of phenol to cyclohexanone*	[118]
Pd@CN$_{600}$	ZIF-67	*Hydrogenation of phenol to cyclohexanone*	[119]
M-dabcotpa@C-800	M-(dabco)(tpa) MOFs. (M=Fe, Mn, Co, Ni, or Cu)	*Amination of aryl, heteroaryl or aliphatic aldehydes*	[120]
Ru SAs/N−C o Ru NCs/C	UiO-66 (Zr$_6$O$_4$(OH)$_4$(bdc)$_6$	*Hydrogenation of quinoline*	[121]
Miscellaneous			
N-doped NPC-Pd	Al-(NH$_2$-bdc)	*Suzuki-Miyaura coupling reaction*	[122]
APC-750@Pd	Zn-based ZIF		[123]
Ni (Ni/NC)	(FA/NH$_4$OH/Ni-MOF-74)	*1,2-dichloroethane to ethylene*	[124]
Pd/Ni-mCN	Ni-MOF	*Hydrodechlorination of 4-chlorophenol*	[125]
N-doped carbons (N=Co, Zn)	ZIF-7, ZIF-8, ZIF-9, and ZIF-67	*CO$_2$ cycloaddition to epoxides*	[126]
ZnO@NPC-Ox	ZIF-8		[127]
CN@MIL	(BmimBr)/MIL-101 (ILs@MIL)	*Synthesis of cyclic carbonates from epoxides*	[128]
Cu@N-C	Copper(II) bisimidazolate	*Cycloaddition reaction to 1,2,3-triazole*	[129]
N-doped porous carbon (Cz-MOF-253)	MOF-253	*Knoevenagel condensation reaction between benzaldehyde and malononitrile*	[130]
Co-ZrO$_2$/N−C	UiO-66-NH$_2$	*Synthesis of quinazolinones from cyclic amines and 2-aminoarylmethanols*	[131]
M$_a$N$_4$/M$_b$N$_4$@NC (M$_a$=Cu, Co, Ni, Mn; M$_b$ = Co, Cu, Fe)	Metallic ZIFs	*Synthesis of flavone derivatives*	[132]

bdc: 1,4-benzenedicarboxylate; **BmimBr**: 1-butyl-3-methylimidazolium bromide; **btc**: 1,3,5-benzenetricarboxylate; **BPY**: 4,4-bipyridine; **dabco**: triethylenediamine; **DYC**: dicyandiamide; **fa** = furfuryl alcohol; **PVP**: polyvinylpyrrolidone; **ted**: triethylenediamine; **tpa**: terephthalic acid; **tpt**: 2,4,6-tris(4-pyridyl)-1,3,5-triazine.

4.3.1. Oxidation Reactions

Oxidation reactions have been widely reported, as anticipated, including oxidation of alcohols and alkanes, olefin epoxidations (Table 3).

Oxidation of alcohols: Especially interesting is the study of Co *N*-doped porous carbons for the aerobic and selective oxidation of 1-phenylethanol, as secondary alcohol, to acetophenone. Bai et al. [97] used the MOF 1, Co$_9$(btc)$_6$(tpt)$_2$(H$_2$O)$_{15}$,·containing different organic linkers. To avoid the nanoparticle aggregation, MOF 1 was gradually pyrolyzed at temperatures varying from 500 to 900 °C, leading to Co/C–N composites with high Co loadings, in which Co nanoparticles were uniformly dispersed. It was observed that the Co/C–N700 sample showed a higher content of pyridinic functions at the surface that could interact with single Co atoms more than in other samples carbonized at higher temperatures, Co/C–N800 and Co/C–N900. Co/C–N catalysts were highly active in the aerobic oxidation of a plethora of differently substituted secondary alcohols selectively (up to 99%) yielding the corresponding ketone in conversions ranging from 67–99%.

Chen et al. [98] developed an easy synthetic approach by direct pyrolysis of hollow Zn/Co-ZIF precursor, at 800 °C, to obtain magnetic separable Co@C−N with high-developed mesoporosity. Co@C−N-800 presented a hollow yolk−shell structure comprising a core constituted by highly dispersed Co^0-doped C−N nanosheets and *N*-doped graphite carbon, in which C and N are homogeneously distributed as shell. The high dispersion of Co nanoparticles was then favored by the strong interactions with both C−N nanosheets and *N*-doped graphite, notably enhancing the catalytic performance for the aerobic oxidation of 1-phenyl ethanol to acetophenone in the absence of any base, in water, at

110 °C. It seems that shell thickness influenced the catalytic performance in such a manner that the Co@C−N(1)-800 sample with medium shell thickness showed improved catalytic performance. The scope of the methodology was investigated by using several substituted secondary benzylic alcohols giving the corresponding ketones in almost quantitative yields.

Interestingly, Ji et al. [99] reported the synthesis of Ru$_3$/CN, in which small clusters of Ru$_3$ are stabilized by nitrogenated species in *N*-doped porous carbon, active in the oxidation of 2-aminobenzyl alcohol. The synthetic strategy consisted of the encapsulation of Ru$_3$(CO)$_{12}$ during the crystallization process of Zn^{2+} and 2-methylimidazole, affording Ru$_3$(CO)$_{12}$@ ZIF-8 MOF, which was subsequently pyrolyzed at 800 °C. Ru$_3$/CN resulted in high catalytic activity, more than isolated Ru nanoparticles, and chemoselectivity to 2-aminobenzaldehyde obtained in quantitative conversion. The authors also performed theoretical calculations concerning the adsorption of 2-aminobenzyl alcohol in the presence of different models simulating Ru$_3$/CN, atomically dispersed Ru$_1$/CN and Ru nanoparticles. The proposed active configuration in the presence of the Ru$_3$/CN model was that where Ru is coordinated with both amine group and hydroxyl in 2-aminobenzyl alcohol.

Oxidation of alkylbenzene derivatives: Ni and Pd/Cu *N*-doped porous carbons have been investigated for oxidation of alkylbenzene derivatives. Such is the case of Ni@C-N obtained from Ni-bdc-dabco-based MOF by pyrolysis at different temperatures [100]. Ni@C-N presented as micro-, meso-, and macroporous and with a surface area ranging from 100–200 m^2 g^{-1}. The Ni@C-N-900-8h sample showed that pyridinic N and graphitic N functions together highly dispersed Ni nanoparticles composed by crystalline Ni^0, formed by a reduction in Ni^{2+} during the carbonization process. Ni@C-N catalysts were tested for ethylbenzene oxidation, under mild conditions, at 80 °C, in the presence of TBHP as oxidant, the catalytic activity being influenced by pyrolysis temperature and time in such a manner that samples obtained at higher temperatures, during short times, showed increased activities (Ni@C-N-900-8h led to acetophenone in 77% of conversions after 48 h). Several alkane derivatives were transformed to the corresponding ketones with good-to-excellent conversions and high selectivity (up to 95%).

A different strategy has been followed by Zhong et al. [101], who reported a Pd–Cu alloy supported by hollow nitrogen-doped carbon materials (Pd–Cu@HO-NPC), derived from a water-sensitive MOF consisting of HKUST-1 coated by an imidazolium-based ionic polymer (ImIP), as a study of proof of concept (Scheme 8).
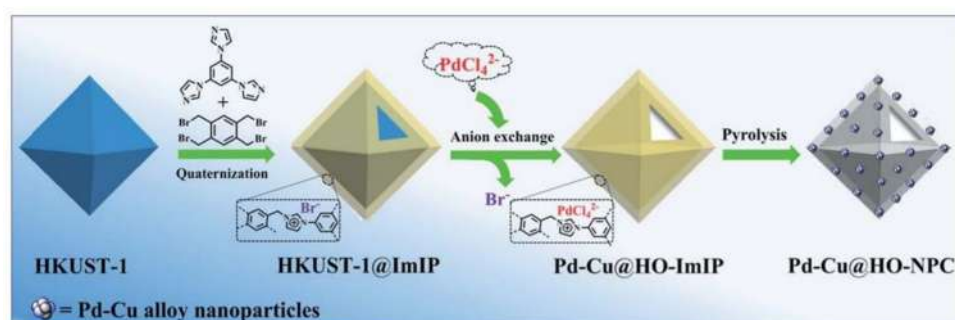
Scheme 8. Synthesis of Pd−Cu@HO−NPC. Reproduced with permission from [101]. Copyright © 2018 Royal Society of Chemistry.

Pd–Cu@HOImIP presented a hollow octahedral structure, shape, and size of the inner cavity coinciding with that from HKUST-1, without structural collapse or structural deformation. Pd–Cu@HO-NPC catalysts showed an analogous hollow octahedral morphology with Pd–Cu alloy nanoparticles homogeneously embedded in the porous carbon shell. It is important to note that the Pd and Cu distributions are identical, suggesting the formation of bimetallic Pd–Cu alloy nanoparticles. Pd–Cu@HO-NPC with a high graphitization degree and Pd-Cu alloy as zero-valent metals and Pd^{2+} and Cu^{2+} at the surface showed high catalytic performance in the aerobic oxidation of hydrocarbons at 120 °C. The presence of

mesopores in Pd–Cu@HO-NPC together with large hollow cavities resulted in being key to the accessibility of active catalytic sites and rapid diffusion of both reactants and products.

Olefin epoxidation: Epoxidation reactions of olefins catalyzed by Co *N*-doped porous carbons, C-N-Co (ZC-700) [102] and Co-CoO@C-N [103] from ZIF-67 and Zn/Co-ZIF, respectively, have been also reported. The use of bimetallic MOF, particularly Zn/Co-ZIF (Zn and Co show similar electronegativity and ionic radius), is considered an interesting synthetic strategy to prepare *N*-doped porous carbons containing Co and CoO nanoparticles. It is possible that in the thermal Zn removal, Co atoms stay anchored to nitrogen at the carbon surface and then prevent the aggregation of Co; the size of Co and CoO nanoparticles ranged from 3~12 nm for the Zn_1Co_1-ZIF derivative. In this case, styrene was transformed in higher conversions at around 99% and with higher selectivity (approx. 70%) in comparison with MOF precursors.

4.3.2. Oxidative Esterification of Alcohols

MOF-derived cobalt *N*-doped carbon materials have been reported for the cross-esterified oxidative reactions between alcohols, specifically benzyl alcohol and methanol. Zhou et al. [104] reported a cobalt MOF (ZIF-67) that can be thermally transformed into Co-CoO@N-doped porous carbon nanocomposites, varying both the pyrolysis temperature and time. Highly dispersed cobalt nanoparticles on *N*-doped porous carbon are mainly composed of Co^0 and with small quantities of CoO and Co-OH covering the outer surface available on the carbon matrix. The NC-700-3h catalyst is presented as uniform concave nanocubes in which Co, C, N, and small amounts of oxygenated species are homogeneously distributed. NC-700-3h resulted in being particularly active in the cross-esterified oxidative reaction between benzyl alcohol and methanol in the presence O_2 and K_2CO_3 as the oxidant agent and base, respectively, at 80 °C during 24 h, selectively leading to methyl benzoate in quantitative conversions. This methodology was applied to other substituted benzyl alcohols and even to aliphatic alcohols, e.g., ethanol transformed to ethyl acetate, and others. The authors proposed a plausible reaction mechanism for the oxidative esterification of alcohols over Co-CoO@N-doped carbon nanocomposites consisting of (i) oxidation of alcohol to the corresponding aldehyde as rate limiting step, (ii) condensation of aldehyde with alcohol to give the hemiacetal as non-catalyzed reaction, and finally, (iii) a catalytic oxidation step affording the corresponding ester.

In the same context, Zhong et al. [105] reported the synthesis of Co@C-N composites also from ZIF-67 and applied to the oxidative esterification of *p*-nitrobenzyl alcohol in the presence of methanol, under mild reaction conditions (25 °C, air, Co@C-N-800), resulting in high conversions (>99%) to methyl *p*-nitrobenzoate (selectivity > 99%).

4.3.3. Reduction Reactions

Hydrogenation of nitro compounds catalyzed by MOF-derived metal *N*-doped porous carbons have also been widely studied. Some examples of these catalysts used in the presence of H_2 or H_2 donors are showed in Table 3. Subsequent sections summarize other relevant reduction reactions involving several functional groups such as reduction in aldehydes/ketones, nitriles, and hydrocarbons, among others.

Reduction in aldehydes/ketones and nitriles: Hydrogenation transfer reactions emerge as sustainable alternatives to the conventional hydrogenations. In this regard, there are reported a few examples of MOF-derived cobalt *N*-doped porous carbons involved in the transfer hydrogenation reaction of α,β-unsaturated carbonylic compounds in the absence of bases. In this context, Co@CN bi-functional catalysts active in the transfer hydrogenation of cinnalmaldehyde, under mild reaction conditions, has been reported [106]. The MOF precursor was $(Co(tpa)(dabco)_{0.5})$ that, after carbonization, yielded *N*-doped carbon layers and supported Co^0 nanocatalysts, mesoporous materials with a large number of basic centers, improving the catalytic performance without the presence of bases. Those obtained at higher temperatures, Co@CN-900, presented Co^0 nanoparticles with increased sizes located in surroundings of carbon layers. In this case, Co@CN-900 was found to be the best catalyst

when using *n*-hexanol as the hydrogen donor, affording cinnamal alcohol in quantitative conversion and excellent selectivity (99%) and also exhibiting a great recyclability.

Chen et al. [113] developed a hydrophilic *N*-doped porous carbon able to stabilize highly dispersed Pd nanoparticles via an incipient-wetness impregnation method, using H_2PdCl_4 aqueous solutions, and subsequent reduction with H_2. The NPC-ZIF-8-900 used as support was obtained by pyrolysis of ZIF-8 at 900 °C, resulting in a porous carbon containing N uniformly dispersed, without the presence of Zn species and showing high surface area. The authors assumed that micropores and N in NPC-ZIF-8-900 allowed the good dispersion of Pd nanoparticles. The Pd/NPC-ZIF-8 catalyst efficiently promoted the dehydrogenation of vanillin, in water under H_2 atmosphere at 90 °C, leading to the desired product in quantitative conversion and total selectivity (Scheme 9).
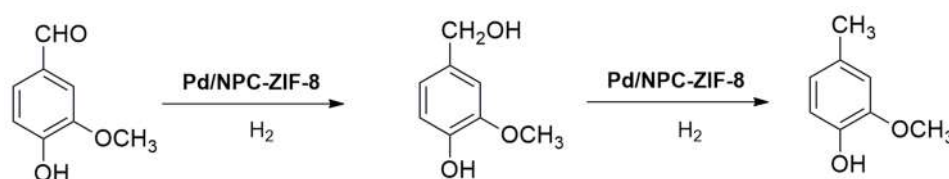
**Scheme 9.** Dehydrogenation of vanillin catalyzed by Pd/NPC-ZIF-8.

Reduction in ketones either by hydrogenation or hydrosilylation is a relevant and extensively used transformation for fine chemicals production. Long et al. [114] reported similar Co@C-N catalysts from (Co(bdc)(ted)$_{0.5}$) by pyrolysis at different temperatures. In this case, Co@C-N catalysts were applied in transfer hydrogenation reactions by using different functionalized compounds including aryl and aliphatic ketones, nitriles, nitro compounds, and even olefins, in the presence of isopropanol at 80 °C. Co@C-N-900-15h resulted on the best catalytic performance leading to the desired product in good to excellent conversion (80–99%) and selectivity up to 90%. The Co@C-N-900 catalyst was able to selectively catalyze the transfer hydrogenation reaction of nitriles to primary amines or imines with controllable selectivity (up to 90%) as a function of the hydrogen donor volume, isopropanol, in such a manner that large amounts of isopropanol promoted the formation of the corresponding benzyl imine [133]. *N*-derived basic sites seem to be also responsible for selectivity. The authors proposed a tentative reaction mechanism for the reaction, as illustrated in Scheme 10. Firstly, the adsorption of the reagents took place over the catalyst surface (**I**). Catalytic basic sites abstracted the proton from isopropanol, this proton activating the benzonitrile (**II**) to give acetone and the primary imine (**III**). The formed imine was subsequently hydrogenated (**IV**) releasing benzylamine (**V**), which reacted with another imine molecule (**III**) affording the intermediate (**VI**). The final desorption of diamine (**VII**) regenerated the catalyst, available for the next cycle, while diamine (**VII**) underwent the NH_3 release affording the corresponding imine (**VIII**).

Following the same methodology, these authors also investigated M/M' alloy nanoparticles embedded in the *N*-doped carbon matrix, where M/M' are Co, Ni, or Cu, for the synthesis of *N*-benzylidenebenzylamine via benzonitrile reduction [115]. Multimetallic MOF, ((M-M'(1,4-bdc)$_2$(dabco)·4DMF·1/2H_2O, M/M'=Co, Ni, Cu), was used as precursor, which by direct pyrolysis, at 500 °C under helium atmosphere, was converted on transition metal alloy nanoparticles highly dispersed at the *N*-doped graphitic carbon surface. Among the investigated porous carbons, Co-Ni(3:1)@C-N was found to be the most efficient catalyst for the transfer hydrogenation of a plethora of substituted nitriles to the corresponding *N*-benzylidenebenzylamines in high conversions (up to 98%) and selectivity (up to 80%).
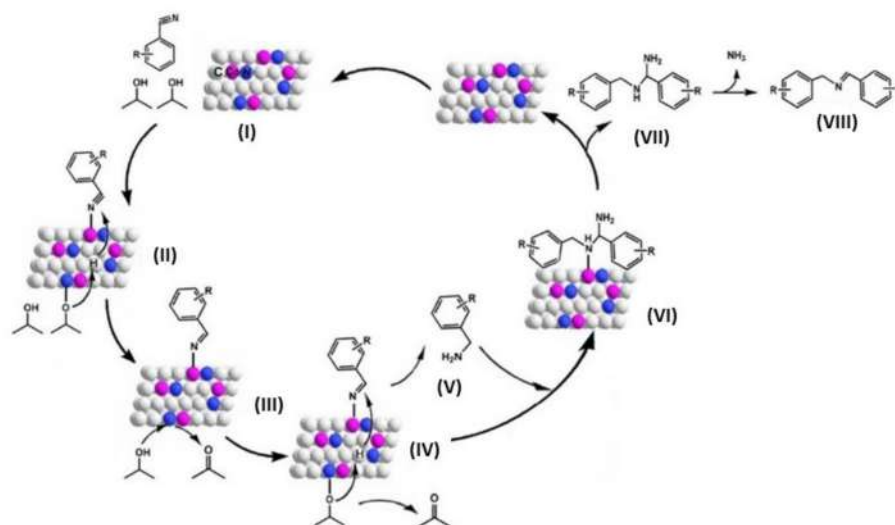
Scheme 10. Proposed reaction mechanism for the transfer hydrogenation of nitriles to primary amines and imines. Reproduced with permission from ref. [133]. Copyright © 2017, American Chemical Society.

Concerning the catalytic hydrosilylation of ketones, Bennedsen et al. [116] reported on alloy Co-Ni nanoparticles encapsulated in porous carbon (CoNi@NC$_x$), prepared by impregnation of cobalt *N*-doped graphitic porous carbon derived from ZIF-67 with nickel(II) nitrate, by using the incipient wetness impregnation method and subsequent carbonization at different temperatures. CoNi@NC$_{800}$ was composed by alloy Co-Ni nanoparticles in 67% (Co/Ni ratio = 60:40), being a mesoporous material with diminished BET surface area regarding its Co carbon precursor (Co@NC$_{800}$) (213 vs. 283 m^2 g^{-1}). CoNi@NC$_{800}$ was the most efficient catalyst for the hydrosilylation of cyclohexanone with Me$_2$PhSiH, in heptane, at 90 °C, affording the desired product in quantitative conversion and selectivity after 24 h of reaction time (Scheme 11).
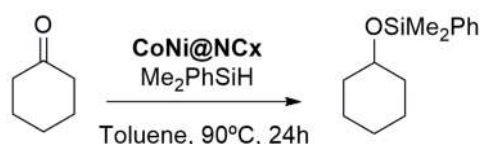

Scheme 11. Hydrosilylation of cyclohexanone with Me$_2$PhSiH.

Other reduction reactions: Other reduction reactions have been also studied and are succinctly commented on in this section and summarized in Table 3.

Li et al. [117] used a magnetic and highly porous carbon, derived from ZIF-67, to support well-dispersed Pd nanoparticles in different loadings (Pd-MDPC). Magnetically separable Pd-MDPC(2.39) catalyst was highly active and selective in the semihydrogenation of terminal alkynes to olefins, in methanol as solvent, in the presence of H$_2$ at 25 °C. In the same context, Ding et al. [118] developed a series of highly active Pd@CN catalysts by using additional nitrogen sources such as DICY or PVP during the ZIF-67 synthesis. Notable differences regarding the catalyst structure were found, therefore also influencing the catalytic performance in the phenol hydrogenation. The use of DICY produced an increase in the surface area but also of nitrogen content, preventing the oxidation of the Pd^0 nanoparticles and then resulting in porous carbons (Pd@CN$_D$) with higher Pd^0 loading. Pd@CN$_D$ was the most active and reusable catalyst for the hydrogenation of phenol to cyclohexanone in 96% of conversions and 94% of selectivity. The high N content in the Pd@CN$_D$ catalyst favored the phenol adsorption by hydrogen binding, whereas activated H$_2$ by Pd^0 nanoparticles reduced the benzene ring. The weak interactions of cyclohexanone with the catalyst did not favor its hydrogenation.

A similar strategy to develop Pd nanoparticles supported on *N*-doped porous carbons has been used by Ding et al. [119]. Pd@CN$_{600}$ *N*-doped mesoporous carbon, prepared also from ZIF-67, was found to be a reusable catalyst able to promote the hydrogenation of phenol to cyclohexanone, in water, in the presence of H$_2$ at 80 °C, in high conversion (95%) and selectivity (95%).

Interestingly, Jagadeesh et al. [120] described the reductive amination of aryl, heteroaryl, or aliphatic aldehydes with NH$_3$ and H$_2$ promoted by cobalt nanoparticles encapsulated by graphitic shell catalysts (Scheme 12).
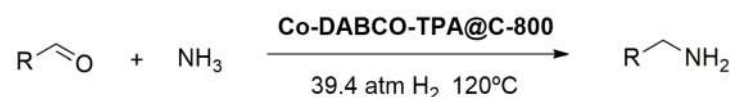

Scheme 12. Reductive amination of aldehydes catalyzed by Co-DABCO-TPA@C-800.

Catalysts were prepared from M-(dabco)(tpa) MOFs, where M is Fe, Mn, Co, Ni, or Cu, immobilized on commercial Vulcan XC 72R carbon, and subsequent pyrolysis as shown in Scheme 13. Catalytic performance of these catalysts (M-dabcotpa@C-800) were checked in the reductive amination of 3,4-dimethoxybenzaldehyde to 3,4-dimethoxybenzylamine as part of several molecules with biological activity. Co-dabcotpa@C-800 resulted in the best catalytic performance yielding the desired amine in 88%, whereas the rest of the samples acting with notably lower activity also compared with the corresponding carbon catalyst from isolated MOFs. Co-dabcotpa@C-800 is composed of cobalt species consisting of Co^0 nanoparticles (5–30 nm) at the graphitic layers but also Co$_3$O$_4$ in considerable smaller quantity or even single Co atoms. As already anticipated, the pyrolysis temperature was a key factor in the catalytic performance in such a manner that the Co-DABCOTPA@C-600 sample contained higher Co^0 loading beside the formation of elementary graphitic shells. The developed methodology was also successfully extended to the reductive amination to give the corresponding secondary or even tertiary amines.
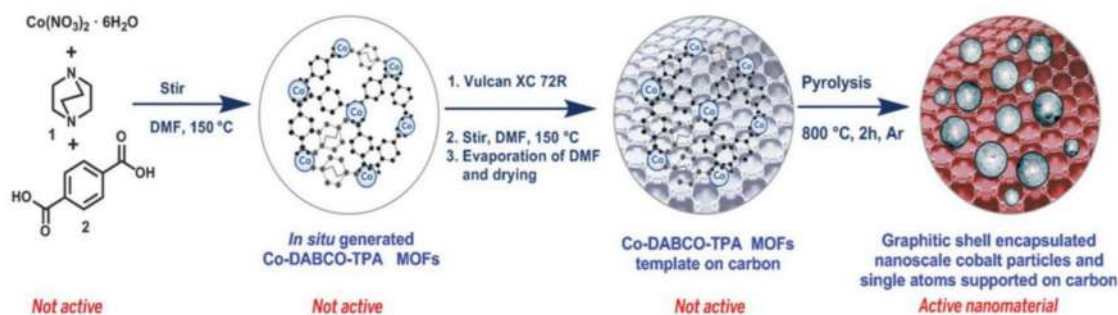
Scheme 13. Preparation of graphitic-shell-encapsulated Co nanoparticles supported on carbon by using MOF precursors. Reproduced with permission from [120]. Copyright © 2017, The American Association for the Advancement of Science.

Especially interesting is the synthesis of *N*-porous carbons in which single Ru atoms are supported, reported by Wang et al. [121]. The used MOFs were UiO-66 (Zr$_6$O$_4$(OH)$_4$(bdc)$_6$) and its amine functionalized MOF (UiO-66 UiO-66−NH$_2$). The synthetic strategy consisted of merging RuCl$_3$ during the MOF synthesis, demonstrating the interaction of Ru with amine groups in UiO-66 UiO-66−NH$_2$. Subsequent pyrolysis at 700 °C yielded porous carbons (Ru SAs/N−C or Ru NCs/C) with large pore volume and surface area composed by Ru^{3+} species comprising Ru single atoms or small Ru clusters and small ZrO$_2$ crystals removed by etching with HF solution. Remarkably, Ru SAs/N−C resulted in being highly active in the hydrogenation of quinoline, in the presence of H$_2$ at 100 °C, to tetrahydroquinoline in high both conversion (99%) and selectivity (99%) (Scheme 14).
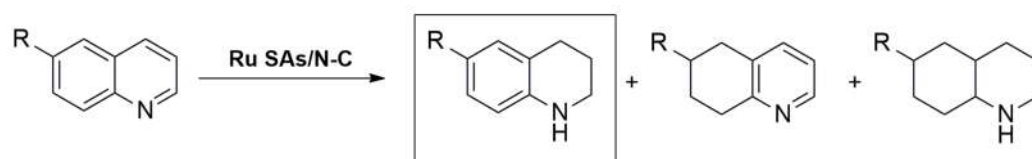
Scheme 14. Synthesis of 1,2,3,4-tetrahydro quinolines catalyzed by Ru SAs/N–C catalyst.

4.3.4. Cross-Coupling Reactions

Zhang et al. [122] reported a new catalyst for the Suzuki–Miyaura coupling reaction, under mild conditions, consisting of well-dispersed Pd^0 nanoparticles supported on the *N*-decorated nanoporous carbon derived from Al-(NH_2-bdc). The *N*-doped NPC-Pd composite presented a BET surface area of $600 \ m^2 \ g^{-1}$ and a porous structure, including from micropores to macropores, in which the presence of Al_2O_3 could help to stabilize the Pd nanoparticles. *N*-doped NPC-Pd was applied to the coupling of a great variety of substituted aryl boronic acids and aryl halides, in mixtures $EtOH$-H_2O as solvent, and in the presence of K_2CO_3 at 25 °C, affording the corresponding biphenyls in high yields (up to 90%) after short reaction times (0.5–1 h). Much more recently, Bugday et al. [123] have reported a Pd-doped *N*-doped carbon (APC-750@Pd) prepared from a Zn-based ZIF, produced by assembly of zinc nitrate hexahydrate and 5,6-dimethylbenzimidazole. Zn-based ZIF was submitted to thermal treatment, at 1000 °C, and activated with KOH, giving rise to APC-750 as support used for $PdCl_2$ impregnation and subsequent reduction with $NaBH_4$ (APC-750@Pd^0). This catalyst was used in the Suzuki–Miyaura cross-coupling reaction between different boronic acids and aryl bromides, in the presence of K_2CO_3, using mixtures of isopropanol-H_2O as solvent, at 50–80 °C, affording the corresponding biphenyls with good-to-excellent yields at notably short reaction times (5–60 min).

### 4.3.5. Hydrodechlorination Reactions

Ni-*N*-doped porous carbons involved in hydrodechlorination reactions have been also reported. Ning et al. [124] have recently developed a *N*-doped carbon-supported Ni (Ni/NC) prepared by direct pyrolysis of Ni-MOF-74 modified with furfuryl alcohol (FA) and NH_4OH (FA/NH_4OH/Ni-MOF-74) at 450 or 600 °C. This modification was effective to increase the Ni nanoparticles' dispersion because of the strong interactions with the support, mainly composed of Ni^0 but also NiO and Ni(OH)$_2$. Ni/NC catalysts were assayed in the gas-phase selective hydrodechlorination reaction of 1,2-dichloroethane to ethylene resulting in superior catalytic performance to non-*N*-doped catalysts. Ni/NC-450 was found to be the most efficient catalyst, demonstrating the importance of both the pyrolysis temperature and *N*-doping.

Cui et al. [125] reported a bimetallic MOF-derived *N*-doped magnetic mesoporous carbon (Pd/Ni-mCN) from Ni-MOF where Ni is coordinated to two different organic linkers, 4,4-bipyridine and BTC. The authors used Ni-mCN carbon obtained by pyrolysis (700 °C) as support of Pd nanoparticles. Zero-valent Ni nanoparticles exhibiting good crystallinity were well-dispersed on the mCN framework, whereas a fraction of Pd as Pd^{2+} dispersed at the surface of the mesopores. Pd/Ni-mCN was able to efficiently catalyze the catalytic hydrodechlorination of 4-chlorophenol, in water in the presence of H_2 and NaOH as base, at 20 °C, affording phenol in almost quantitative yields. Pd/Ni-mCN showed high catalytic activity when using other chlorophenol derivatives.

4.3.6. Cycloaddition Reactions

CO_2 cycloaddition reactions: *N*-doped carbons containing metals prepared from ZIFs—ZIF-7, ZIF-8, ZIF-9, and ZIF-67—by direct pyrolysis at different temperatures have been investigated in the CO_2 cycloaddition to epoxides at 80 °C [126]. Among them, the C600-ZIF-9 catalyst, which presented the highest N content (10.8 wt%), and the Co nanoparticles at the *N*-doped carbon surface, mainly composed of Co^0 but also partially oxidized at the outer surface, exhibited the best catalytic performance, yielding the corresponding

carbonate in 90% after 6 h of reaction time (Scheme 15). Remarkably, Co^0 or even other Co phases such as CoO, Co_3O_4, and ZnO resulted in being barely active for this transformation. Furthermore, C600-ZIF-9 showed the presence of acid and basic sites that could act in cooperation, promoting the reactant adsorption and catalyzing efficiently the reaction.
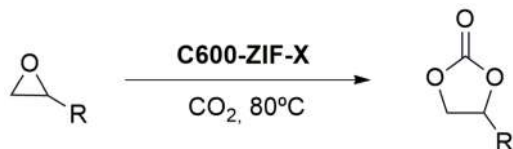

Scheme 15. Synthesis of cyclic carbonates from CO_2 and epoxides.

Ding et al. [127] also investigated *N*-doped porous carbons with encapsulated ZnO nanoparticles (ZnO@NPC-Ox), obtained from ZIF-8 by thermal treatment under inert atmosphere and subsequent oxidation in the presence of sodium hypochlorite, which showed diverse oxygenated functions at the surface such as carboxylic acids, phenols, and lactones. Well-dispersed ZnO at the surface in ZnO@NPC-Ox-700 was notably diminished after oxidant treatment, almost disappearing for ZnO@NPC-Ox-800. ZnO@NPC-Ox samples presented BET surface areas notably lower than their porous carbon precursors (77–150 vs. 403–1963 m^2 g^{-1}) because of the presence of macropores and also originated by oxidation, making accessible the active catalytic sites. ZnO@NPC-Ox exhibited high catalytic performance for CO_2 cycloaddition reaction with different epoxides, in the presence of tetra butyl ammonium bromide (TBAB), at 60 °C, leading to cyclic carbonates in high conversions (up to 80%) and excellent selectivity (>99%). Particularly, the ZnO@NPC-Ox-700 catalyst presented the best catalytic activity attributed to the presence of ZnO.

Much more recently, Chen et al. [128] investigated a new synthetic approach to prepare mesoporous metal *N*-doped nanocarbon (CN@MIL) and multi-active sites from encapsulated 1-butyl-3-methylimidazolium bromide (BmimB)/MIL-101 precursors (ILs@MIL) by controlled pyrolysis. Porosity of the samples varied depending on the BmimB loadings (w), pyrolysis temperature, and time. All CN@MIL(400, w, 30) materials, which were obtained by pyrolysis at 400 °C during 30 min, presented a sponge-like structure, while the CN@MIL(400, 0.67, 30) sample showing superior mesopore volume. The CN@MIL catalysts were tested for the synthesis of cyclic carbonates from epoxides and ambient pressure of CO_2 at 90 °C, obtained in good to excellent conversions. Cr^{3+} and Br^- as Lewis acids or Lewis bases, respectively, together with the great affinity toward CO_2, are probably behind the excellent catalytic performance.

Click chemistry reactions: 1,2,3-Triazole is a heterocyclic system as part of several biological biologically active compounds. Regarding this, Wang et al. [129] reported the one-pot 1,3-dipolar cycloaddition of terminal alkynes, aryl halides, and sodium azide promoted by reusable Cu@N-C catalysts as MOF-derived porous carbons. The MOF precursor was the copper(II) bisimidazolate $(Cu(im)_2)$ pyrolyzed at different temperatures (400, 600, and 800 °C) under argon atmosphere. Cu@N-C composites showed similar crystal structures increasing the Cu^0 content when increasing the pyrolysis temperature. Cu@N-C catalysts exhibited high catalytic performance in the cycloaddition reaction between benzyl bromide, sodium azide, and phenylacetylene in water or $^tBuOH/H_2O$ at 50 °C, Cu@N-C (600) sample being the most efficient catalyst leading to the corresponding 1,2,3-triazole in high yield (>94%). The authors used the developed methodology to obtain differently substituted 1,2,3-triazoles in high yields (up to 70%), even derivatizing complex molecules (Scheme 16).
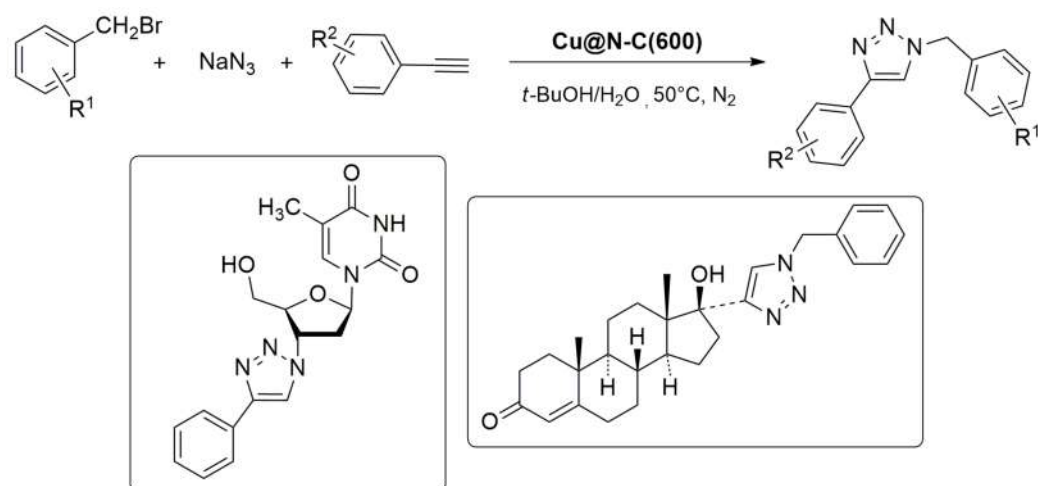
Scheme 16. 3-Dipolar cycloaddition of terminal alkynes, aryl halides, and sodium azide catalyzed by Cu@N-C(600).

4.3.7. Acid-Base Catalyzed Reactions

As mentioned above, the use of MOF-derived carbon catalysts has been widely investigated in oxidation-reduction reactions. However, as far as we know, only a couple of examples of them have been investigated catalyzing acid-base reactions. Concerning this, Li et al. [130] published for the first time a series of basic *N*-doped porous carbon (Cz-MOF-253) by direct pyrolysis, at different temperatures, of MOF-253, where Al^{3+} is coordinated to 2,2′-bipyridine-5,5′-dicarboxylic acid; Al^{3+} was removed by treatment with HF. Cz-MOF-253 catalysts were tested in the Knoevenagel condensation reaction between benzaldehyde and malononitrile, pyrolysis temperature influencing the catalytic performance. Cz-MOF-253-800, pyrolyzed at 800 °C, presenting medium to strong Lewis basic sites, showed excellent catalytic activity. More interesting was the development of a bifunctional catalyst consisting of Cz-MOF-253-supported Pd nanoparticles (Pd/Cz-MOF-253-800) and applied to the tandem catalytic Knoevenagel condensation–hydrogenation reactions between substituted benzaldehydes with malononitrile, in toluene, to desired products in quantitative conversions with total selectivity (Scheme 17).
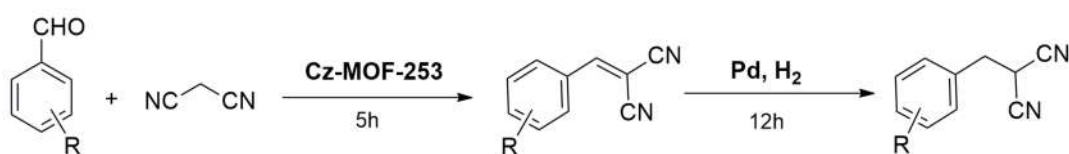
Scheme 17. Knoevenagel condensation–hydrogenation reactions between substituted benzaldehydes and malononitrile promoted by Pd/Cz-MOF-253-800 catalyst.

In the same context, Xie et al. [131] reported the synthesis of quinazolinones from cyclic amines and 2-aminoarylmethanols catalyzed by an MOF-derived carbon catalyst with highly dispersed cobalt nanoparticles at ultralow loadings. The synthetic strategy consisted of starting from UiO-66-NH$_2$, where both $ZrCl_4$ and 2-aminoterephthalic acid (H_2BDC-NH$_2$) were assembled, while $Co(NO_3)_2 \cdot 6H_2O$ and dabco were introduced into the MOFs through an in situ impregnating method. Amine groups in both H_2BDC-NH$_2$ and dabco acted as coordinating agents to cobalt ions then avoiding the aggregation during the thermal treatment at 800 °C. The obtained Co-ZrO$_2$/N−C *N*-doped porous carbon was a microporous–mesoporous sample containing Co^0 nanoparticles homogeneously dispersed and embedded in a *N*-porous matrix but also ZrO$_2$ nanoparticles. A Co-ZrO$_2$/N−C catalyst was tested in the dehydrogenative cross-coupling of both substituted 1,2,3,4-tetrahydroisoquinoline and 2-aminobenzyl alcohols, at 120 °C, in the presence of molecular O$_2$ and 4-nitrobenzoic acid as acid additive and in *p*-xylene, affording the corresponding

quinazolone in moderated yields (41–78%) (Scheme 18). This methodology was also extended to other cyclic amines including 4-methylpiperidine, azepane, and pyrrolidine, tolerating a great variety of functional groups on 2-aminobenzyl alcohols.
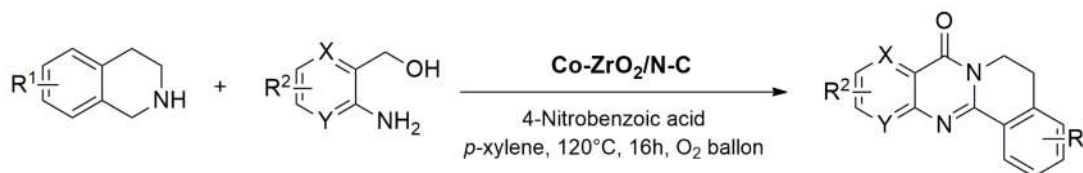
Scheme 18. Synthesis of quinazolones by dehydrogenative cross-coupling of substituted 1,2,3,4-tetrahydroisoquinoline and 2-aminobenzyl alcohols catalyzed by Co-ZrO$_2$/N−C catalyst.

Much more recently, Zhao et al. [132] reported a new strategy to prepare a series of metal SACs embedded on N-doped carbons (M$_a$N$_4$/M$_b$N$_4$@NC where M$_a$=Cu, Co, Ni, Mn and M$_b$=Co, Cu, Fe), derived from metallic ZIFs. SACs were synthetized by using mixtures of M$_a$-based ZIF-8 and M$_b$-based phthalocyanine (Ph) pyrolyzed in the presence of mixed molten salt (KCl-KBr) to yield M$_a$N$_4$/M$_b$N$_4$@NC porous carbons, in which both M$_a$N$_4$ and M$_b$N$_4$ sites are homogeneously distributed. Particularly, CuN$_4$/CoN$_4$@NC showed high catalytic activity in the domino synthesis of flavone derivatives, from differently substituted benzaldehydes and 2′-hydroxyacetophenones, using n-hexanol as a solvent, in the presence of O$_2$, at 140 °C, to give the corresponding flavone good to excellent yields (70–99%) (Scheme 19). Considering both experimental and theoretical results by using density functional theory (DFT), the authors demonstrated that the observed reactivity of CuN$_4$/CoN$_4$@NC could be due to the synergic effect of both the CuN$_4$ and CoN$_4$ sites reducing the energy barriers for O$_2$ activation and 2′-hydroxyacetophenone transformation, in such a manner that first occurred the condensation between reactants, followed by cyclization to the corresponding flavanone, which underwent an oxidative dehydrogenation.
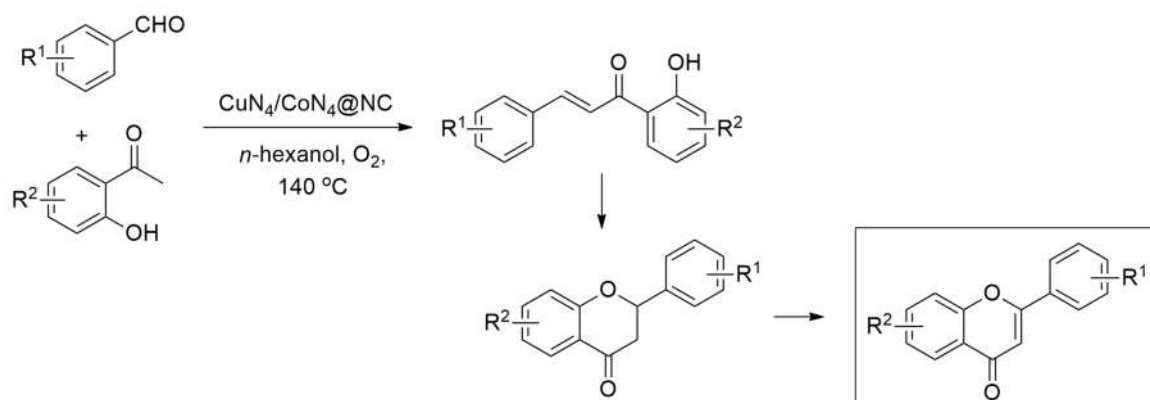
Scheme 19. Synthesis of flavones catalyzed by CuN$_4$/CoN$_4$@NC.

5. Concluding Remarks

Carbon-based materials have been recognized as interesting alternative sustainable catalysts used during recent decades and widely explored in fine chemical synthesis [134,135]. A great variety of doped-carbon catalysts, including metals but also heteroatoms or even both, applied to different research fields and particularly involved in producing highly valuable compounds with high catalytic performance, have been investigated. Among the most investigated and the oldest carbon catalysts are the activated carbons, but also carbon allotropes such as carbon nanotubes, fullerenes, carbon fibers, and even graphene and nanostructured carbons acquiring importance in catalysis almost from discovery. All of them present several limitations such as the accessibility of active sites but also diffusion

problems for both reactants and products. In the case of metal-doped carbon catalysts, an issue to be considered is the metal dispersion intimately related with the surface area, metal loadings, and carbonization temperature. Remarkably, both heteroatom doping and structural defects are then key to improving the metal interactions with the carbon surface favoring both metal stabilization and dispersion. Among the current trends, highlighted is the small-size limit of the metal particles required for the development of SACs, in which single atoms are dispersed over the carbon surface, then maximizing the metal efficiency. It is a fact that MOFs are considered as ideal platforms to prepare SACs.

In the last decade, the use of MOFs as precursors of porous carbons with enhanced catalytic performances, in comparison with other traditional carbonaceous catalysts, is gaining much attention. It is an area of expansion rapidly growing. The great structural diversity of MOFs that can be obtained, with different geometries and sizes becoming infinite possibilities, allows the preparation of a wide variety of functional porous carbons with different compositions, morphologies, and textures as a function of a specific use, including metal-free, metal-doped porous carbons that can be used as both catalysts and catalyst supports. Different methodologies to produce MOF-derived porous carbons, comprising the direct pyrolysis under inert atmosphere of the corresponding MOF, previously prepared or in situ generated in the presence of additional carbon or heteroatom sources or even other supports, have been reported. Although this general strategy is successfully used, the obtained porous carbons present some limitations such as the intrinsic microporous nature but also the irreversible formation of metal nanoparticle aggregated as a consequence of the carbonization process. In this context, new strategies to develop nanoarchitectured carbon materials derived from MOFs as yolk–shell, hollow-porous, mesoporous, and even multidimensional structures are being designed [136].

The use of bimetallic MOFs, particularly those containing Zn species, offers the possibility of controlling the aggregation of the metal nanoparticles. On one side, the presence of Zn can serve to separate vicinal metal atoms but also to develop new porosity after removal either by evaporation or after acidic treatment.

Although the last decade was marked by the great advances concerning the development and properties of MOF-derived porous carbons, much more effort should be focused on the relationship of the synthesis conditions and the final characteristics—morphology, structure, and composition—of the porous carbons as determinant factors conditioning the catalytic performance. Considering that 1D and 2D porous carbons show several advantages, new approaches for their synthesis should be developed in the near future. In addition, it would be an urgent necessity for the development of more sustainable synthetic methods to upscale MOF-derived porous carbons to their industrial implementation.

Finally, it is a reality that MOF-derived porous carbons can be considered good and promising candidates to produce highly valuable compounds. As shown in this review, the most-explored reactions mainly comprise oxidation and reduction reactions, although some examples of coupling but also multicomponent reactions have also been reported. The development of MOF-derived porous carbons and particularly SACs active in the synthesis of biologically valuable heterocyclic compounds through cascade reactions is still a challenge.

Author Contributions: Conceptualization, E.P.-M. and I.M.; writing—original draft preparation, E.P.-M., M.G.-O., I.M. and M.B.; writing—review and editing, E.P.-M., M.G.-O., I.M. and M.B.; supervision, E.P.-M. and I.M.; funding acquisition, E.P.-M., M.G.-O. and I.M. All authors have read and agreed to the published version of the manuscript.

Conflicts of Interest: The authors declare no conflict of interest.

References

1. Stock, N.; Biswas, S. Synthesis of Metal-Organic Frameworks (MOFs): Routes to Various MOF Topologies, Morphologies, and Composites. *Chem. Rev.* **2012**, *112*, 933–969. [CrossRef] [PubMed]
2. Wang, Z.; Liu, L.Y.; Li, Z.; Goyal, N.; Du, T.; He, J.X.; Li, G.K. Shaping of Metal-Organic Frameworks: A Review. *Energy Fuels* **2022**, *36*, 2927–2944. [CrossRef]
3. Wen, Y.H.; Zhang, J.; Xu, Q.; Wu, X.T.; Zhu, Q.L. Pore surface engineering of metal-organic frameworks for heterogeneous catalysis. *Coord. Chem. Rev.* **2018**, *376*, 248–276. [CrossRef]
4. Ferey, G. Hybrid porous solids: Past, present, future. *Chem. Soc. Rev.* **2008**, *37*, 191–214. [CrossRef] [PubMed]
5. Furukawa, H.; Cordova, K.E.; O'Keeffe, M.; Yaghi, O.M. The Chemistry and Applications of Metal-Organic Frameworks. *Science* **2013**, *341*, 1230444. [CrossRef]
6. Gonzalez-Rodal, D.; Palomino, G.T.; Cabello, C.P.; Perez-Mayoral, E. Amino-grafted Cu and Sc Metal-Organic Frameworks involved in the green synthesis of 2-amino-4H-chromenes. Mechanistic understanding. *Microporous Mesoporous Mater.* **2021**, *323*, 111232. [CrossRef]
7. Li, J.R.; Ma, Y.G.; McCarthy, M.C.; Sculley, J.; Yu, J.M.; Jeong, H.K.; Balbuena, P.B.; Zhou, H.C. Carbon dioxide capture-related gas adsorption and separation in metal-organic frameworks. *Coord. Chem. Rev.* **2011**, *255*, 1791–1823. [CrossRef]
8. Qazvini, O.T.; Babarao, R.; Telfer, S.G. Selective capture of carbon dioxide from hydrocarbons using a metal-organic framework. *Nat. Commun.* **2021**, *12*, 197. [CrossRef]
9. Fang, Y.X.; Ma, Y.W.; Zheng, M.F.; Yang, P.J.; Asiri, A.M.; Wang, X.C. Metal-organic frameworks for solar energy conversion by photoredox catalysis. *Coord. Chem. Rev.* **2018**, *373*, 83–115. [CrossRef]
10. Olorunyomi, J.F.; Geh, S.T.; Caruso, R.A.; Doherty, C.M. Metal-organic frameworks for chemical sensing devices. *Mater. Horiz.* **2021**, *8*, 2387–2419. [CrossRef]
11. Tchinsa, A.; Hossain, M.F.; Wang, T.; Zhou, Y.B. Removal of organic pollutants from aqueous solution using metal organic frameworks (MOFs)-based adsorbents: A review. *Chemosphere* **2021**, *284*, 131393. [CrossRef]
12. Bavykina, A.; Kolobov, N.; Khan, I.S.; Bau, J.A.; Ramirez, A.; Gascon, J. Metal-Organic Frameworks in Heterogeneous Catalysis: Recent Progress, New Trends, and Future Perspectives. *Chem. Rev.* **2020**, *120*, 8468–8535. [CrossRef] [PubMed]
13. Konnerth, H.; Matsagar, B.M.; Chen, S.S.; Prechtl, M.H.G.; Shieh, F.K.; Wu, K.C.W. Metal-organic framework (MOF)-derived catalysts for fine chemical production. *Coord. Chem. Rev.* **2020**, *416*, 213319. [CrossRef]
14. Lawson, H.D.; Walton, S.P.; Chan, C. Metal-Organic Frameworks for Drug Delivery: A Design Perspective. *ACS Appl. Mater. Interfaces* **2021**, *13*, 7004–7020. [CrossRef]
15. Perez-Mayoral, E.; Matos, I.; Bernardo, M.; Fonseca, I.M. New and Advanced Porous Carbon Materials in Fine Chemical Synthesis. Emerging Precursors of Porous Carbons. *Catalysts* **2019**, *9*, 133. [CrossRef]
16. Perez-Mayoral, E.; Matos, I.; Bernardo, M.; Ventura, M.; Fonseca, I.M. Carbon-Based Materials for the Development of Highly Dispersed Metal Catalysts: Towards Highly Performant Catalysts for Fine Chemical Synthesis. *Catalysts* **2020**, *10*, 1407. [CrossRef]
17. Marpaung, F.; Kim, M.; Khan, J.K.; Konstantinov, K.; Yamauchi, Y.; Hossain, S.S.; Na, J.; Kim, J. Metal–Organic Framework (MOF)-Derived nanoporous carbon materials. *Chem. Asian J.* **2019**, *14*, 1331–1343. [CrossRef]
18. Huang, H.G.; Shen, K.; Chen, F.F.; Li, Y.W. Metal-Organic Frameworks as a Good Platform for the Fabrication of Single-Atom Catalysts. *ACS Catal.* **2020**, *10*, 6579–6586. [CrossRef]
19. Wang, J.; Wang, Y.; Hu, H.; Yang, Q.; Cai, J. From metal-organic frameworks to porous carbon materials: Recent progress and prospects from energy and environmental perspectives. *Nanoscale* **2020**, *12*, 4238–4268. [CrossRef]
20. Bedia, J.; Muelas-Ramos, V.; Peñas-Garzón, M.; Gómez-Avilés, A.; Rodríguez, J.J.; Belver, C. A review on the synthesis and characterization of metal organic frameworks for photocatalytic water purification. *Catalysts* **2019**, *9*, 52. [CrossRef]
21. Qu, W.; Chen, C.; Tang, Z.; Wen, H.; Hu, L.; Xia, D.; Tian, S.; Zhao, H.; He, C.; Shu, D. Progress in metal-organic-framework-based single-atom catalysts for environmental remediation. *Coord. Chem. Rev.* **2023**, *474*, 214855. [CrossRef]
22. Sharanyakanth, P.S.; Radhakrishnan, M. Synthesis of metal-organic frameworks (MOFs) and its application in food packaging: A critical review. *Trends Food Sci. Technol.* **2020**, *104*, 102–116. [CrossRef]
23. Yu, S.; Meng, X.; Li, Z.; Zhang, W.; Ju, X. Heterofullerene C48B12-impregnated MOF-5 and IRMOF-10 for hydrogen storage: A combined DFT and GCMC simulations study. *Int. J. Hydrogen Energy* **2022**, *47*, 39586–39594. [CrossRef]
24. Yusuf, V.F.; Malek, N.I.; Kailasa, S.K. Review on Metal-Organic Framework Classification, Synthetic Approaches, and Influencing Factors: Applications in Energy, Drug Delivery, and Wastewater Treatment. *ACS Omega* **2022**, *7*, 44507–44531. [CrossRef]
25. Soni, S.; Bajpai, P.K.; Arora, C. A review on metal-organic framework: Synthesis, properties and ap-plication. *Charact. Appl. Nanomater.* **2020**, *3*, 87. [CrossRef]
26. Xiang, F.; Marti, A.M.; Hopkinson, D.P. Layer-by-layer assembled polymer/MOF membrane for H2/CO2 separation. *J. Membr. Sci.* **2018**, *556*, 146–153. [CrossRef]
27. Vaitsis, C.; Kanellou, E.; Pandis, P.K.; Papamichael, I.; Sourkouni, G.; Zorpas, A.A.; Argirusis, C. Sonochemical synthesis of zinc adipate Metal-Organic Framework (MOF) for the electrochemical reduction of CO2: MOF and circular economy potential. *Sustain. Chem. Pharm.* **2022**, *29*, 100786. [CrossRef]

28. Kaur, G.; Kandwal, P.; Sud, D. Sonochemically synthesized Zn (II) and Cd (II) based metal-organic frameworks as fluoroprobes for sensing of 2,6-dichlorophenol. *J. Solid State Chem.* **2023**, *319*, 123833. [CrossRef]

29. Zhang, B.; Chen, J.; Fu, Y. Soft Spray: An Emerging Technique for Metal–Organic Framework-Based Materials. *Langmuir* **2022**, *38*, 13635–13646. [CrossRef]

30. Cohen, S.M. Postsynthetic methods for the functionalization of metal-organic frameworks. *Chem. Rev.* **2012**, *112*, 970–1000. [CrossRef]

31. Hu, L.; Chen, J.; Wei, Y.; Wang, M.; Xu, Y.; Wang, C.; Gao, P.; Liu, Y.; Liu, C.; Song, Y.; et al. Photocatalytic degradation effect and mechanism of Karenia mikimotoi by non-noble metal modified TiO2 loading onto copper metal organic framework (SNP-TiO2@Cu-MOF) under visible light. *J. Hazard. Mater.* **2023**, *442*, 130059. [CrossRef]

32. Kumaraguru, S.; Nivetha, R.; Gopinath, K.; Sundaravadivel, E.; Almutairi, B.O.; Almutairi, M.H.; Mahboob, S.; Kavipriya, M.R.; Nicoletti, M.; Govindarajan, M. Synthesis of Cu-MOF/CeO2 nanocomposite and their evaluation of hydrogen production and cytotoxic activity. *J. Mater. Res. Technol.* **2022**, *18*, 1732–1745. [CrossRef]

33. Wang, X.; Rong, Y.; Wang, F.; Zhang, C.; Wang, Q. High performance proton exchange membranes with double proton conduction pathways by introducing MOF impregnated with protic ionic liquid into SPEEK. *Microporous Mesoporous Mater.* **2022**, *346*, 112314. [CrossRef]

34. Boukayouht, K.; Bazzi, L.; Hankari, S.E. Sustainable synthesis of metal-organic frameworks and their derived materials from organic and inorganic wastes. *Coord. Chem. Rev.* **2023**, *478*, 214986. [CrossRef]

35. Zhang, L.; Wang, C.Y.; Wang, C.C. Mining resources from wastes to produce high value-added MOFs. *Resour. Conserv. Recycl.* **2023**, *190*, 106805. [CrossRef]

36. El-Sayed, E.S.M.; Yuan, D. Waste to MOFs: Sustainable linker, metal, and solvent sources for value-added MOF synthesis and applications. *Green Chem.* **2020**, *22*, 4082–4104. [CrossRef]

37. Shanmugam, M.; Chuaicham, C.; Augustin, A.; Sasaki, K.; Sagayaraj, P.J.J.; Sekar, K. Upcycling hazardous metals and PET waste-derived metal-organic frameworks: A review on recent progresses and prospects. *New J. Chem.* **2022**, *46*, 15776–15794. [CrossRef]

38. Zhong, L.; Ding, J.; Qian, J.; Hong, M. Unconventional inorganic precursors determine the growth of metal-organic frameworks. *Coord. Chem. Rev.* **2021**, *434*, 213804. [CrossRef]

39. Arias, J.J.R.; Thielemans, W. Instantaneous hydrolysis of PET bottles: An efficient pathway for the chemical recycling of condensation polymers. *Green Chem.* **2021**, *23*, 9945–9956. [CrossRef]

40. Farahani, S.D.; Zolgharnein, J. Removal of Alizarin red S by calcium-terephthalate MOF synthesized from recycled PET-waste using Box-Behnken and Taguchi designs optimization approaches. *J. Solid State Chem.* **2022**, *316*, 123560. [CrossRef]

41. Ghosh, A.; Das, G. Facile synthesis of Sn(II)-MOF using waste PET bottles as an organic precursor and its derivative SnO2NPs: Role of surface charge reversal in adsorption of toxic ions. *J. Environ. Chem. Eng.* **2021**, *9*, 105288. [CrossRef]

42. Zhang, F.; Chen, S.; Nie, S.; Luo, J.; Lin, S.; Wang, Y.; Yang, H. Waste PET as a Reactant for Lanthanide MOF Synthesis and Application in Sensing of Picric Acid. *Polymers* **2019**, *11*, 2015. [CrossRef] [PubMed]

43. Deleu, W.P.R.; Stassen, I.; Jonckheere, D.; Ameloot, R.; Vos, D.E.D. Waste PET (bottles) as a resource or substrate for MOF synthesis. *J. Mater. Chem. A* **2016**, *4*, 9519–9525. [CrossRef]

44. Karam, L.; Miglio, A.; Specchia, S.; Hassan, N.E.; Massiani, P.; Reboul, J. PET waste as organic linker source for the sustainable preparation of MOF-derived methane dry reforming catalysts. *Mater. Adv.* **2021**, *2*, 2750–2758. [CrossRef]

45. Slater, B.; Wong, S.O.; Duckworth, A.; White, A.J.P.; Hill, M.R.; Ladewig, B.P. Upcycling a plastic cup: One-pot synthesis of lactate containing metal organic frameworks from polylactic acid. *Chem. Commun.* **2019**, *55*, 7319–7322. [CrossRef]

46. Kabtamu, D.M.; Wu, Y.N.; Chen, Q.; Zheng, L.; Otake, K.I.; Matović, L.; Li, F. Facile Upcycling of Hazardous Cr-Containing Electroplating Sludge into Value-Added Metal-Organic Frameworks for Efficient Adsorptive Desulfurization. *ACS Sustain. Chem. Eng.* **2020**, *8*, 11253–11262. [CrossRef]

47. Song, K.; Qiu, X.; Han, B.; Liang, S.; Lin, Z. Efficient upcycling electroplating sludge and waste PET into Ni-MOF nanocrystals for the effective photoreduction of CO2. *Environ. Sci. Nano* **2021**, *8*, 390–398. [CrossRef]

48. Feng, L.; Wang, K.Y.; Willman, J.; Zhou, H.C. Hierarchy in Metal-Organic Frameworks. *ACS Cent. Sci.* **2020**, *6*, 359–367. [CrossRef]

49. Doan, H.V.; Hamzah, H.A.; Prabhakaran, P.K.; Petrillo, C.; Ting, V.P. Hierarchical Metal-Organic Frameworks with Macroporosity: Synthesis, Achievements, and Challenges. *Nano-Micro Lett.* **2019**, *11*, 54. [CrossRef]

50. Duan, C.; Liang, K.; Zhang, Z.; Li, J.; Chen, T.; Lv, D.; Li, L.; Kang, L.; Wang, K.; Hu, H.; et al. Recent advances in the synthesis of nanoscale hierarchically porous metal–organic frameworks. *Nano Mater. Sci.* **2022**, *4*, 351–365. [CrossRef]

51. Duan, C.; Zhang, H.; Li, F.; Xiao, J.; Luo, S.; Xi, H. Hierarchically porous metal–organic frameworks: Rapid synthesis and enhanced gas storage. *Soft Matter* **2018**, *14*, 9589–9598. [CrossRef]

52. Li, R.; Wu, L.; Chang, G.; Ke, S.; Wang, Y.; Yao, Y.; Zhang, Y.; Li, J.; Yang, X.; Chen, B. Solvent-Mediated Synthesis of Hierarchical MOFs and Derived Urchin-Like Pd@SC/HfO2with High Catalytic Activity and Stability. *ACS Appl. Mater. Interfaces* **2022**, *14*, 5887–5896. [CrossRef]

53. Niu, P.; Lu, N.; Liu, J.; Jia, H.; Zhou, F.; Fan, B.; Li, R. Water-induced synthesis of hierarchical Zr-based MOFs with enhanced adsorption capacity and catalytic activity. *Microporous Mesoporous Mater.* **2019**, *281*, 92–100. [CrossRef]

54. Yang, X.; Yan, L.; Kong, X.; Liu, S.; Zhao, X.; Yang, X.; Yan, L.; Liu, S.; Zhao, X.; Kong, X. Metal-Organic-Framework-Based Single-Atomic Catalysts for Energy Conversion and Storage: Principles, Advances, and Theoretical Understandings. *Adv. Sustain. Syst.* **2021**, *6*, 2100281. [CrossRef]

55. Ye, J.; Yan, J.; Peng, Y.; Li, F.; Sun, J. Metal-organic framework-based single-atom catalysts for efficient electrocatalytic CO2 reduction reactions. *Catal. Today* **2023**, *410*, 68–84. [CrossRef]

56. Han, A.; Wang, B.; Kumar, A.; Qin, Y.; Jin, J.; Wang, X.; Yang, C.; Dong, B.; Jia, Y.; Liu, J. Recent Advances for MOF-Derived Carbon-Supported Single-Atom Catalysts. *Small Methods* **2019**, *3*, 1800471. [CrossRef]

57. Hao, M.; Qiu, M.; Yang, H.; Hu, B.; Wang, X. Recent advances on preparation and environmental applications of MOF-derived carbons in catalysis. *Sci. Total Environ.* **2021**, *760*, 143333. [CrossRef]

58. Yang, L.; Zeng, X.; Wang, W.; Cao, D. Recent progress in MOF-derived, heteroatom-doped porous carbons as highly efficient electrocatalysts for oxygen reduction reaction in fuel cells. *Adv. Funct. Mater.* **2018**, *28*, 1704537. [CrossRef]

59. Yang, K.; Yan, Y.; Wang, H.Y.; Sun, Z.X.; Chen, W.; Kang, H.T.; Han, Y.; Zahng, W.Q.; Sun, X.H.; Li, Z.X. Monodisperse Cu/Cu2O@C core-shell nanocomposite supported on rGO layers as an efficient catalyst derived from a Cu-based MOF/GO structure. *Nanoscale* **2018**, *10*, 17647–17655. [CrossRef]

60. Wu, Y.; Xu, H.; Gao, J. Metal-organic framework-derived porous carbon templates for catalysis. In *Emerging Carbon Materials for Catalysis*; Sadjadi, S., Ed.; Elsevier: Amsterdam, The Netherlands, 2021; pp. 73–121. [CrossRef]

61. Kim, H.C.; Huh, S. Porous carbon-based supercapacitors directly derived from metal-organic frameworks. *Materials* **2020**, *13*, 4215. [CrossRef]

62. Liu, D.; Gu, W.; Zhou, L.; Wang, L.; Zhang, J.; Liu, Y.; Lei, J. Recent advances in MOF-derived carbon-based nanomaterials for environmental applications in adsorption and catalytic degradation. *Chem. Eng. J.* **2022**, *427*, 131503. [CrossRef]

63. Chen, Y.-Z.; Zhang, R.; Jiao, L.; Jiang, H.-L. Metal–organic framework-derived porous materials for catalysis. *Coord. Chem. Rev.* **2018**, *362*, 1–23. [CrossRef]

64. Liu, B.; Shioyama, H.; Akita, T.; Xu, Q. Metal-Organic Framework as a Template for Porous Carbon Synthesis. *J. Am. Chem. Soc.* **2008**, *130*, 5390–5391. [CrossRef]

65. Chaikittisilp, W.; Ariga, K.; Yamauchi, Y. A new family of carbon materials: Synthesis of MOF-derived nanoporous carbons and their promising applications. *J. Mater. Chem. A* **2013**, *1*, 14–19. [CrossRef]

66. Chaikittisilp, W.; Hu, M.; Wang, H.; Huang, H.-S.; Fujita, T.; Wu, K.C.-W.; Chen, L.-C.; Yamauchi, Y.; Ariga, K. Nanoporous carbons through direct carbonization of a zeolitic imidazolate framework for supercapacitor electrodes. *Chem. Commun.* **2012**, *48*, 7259. [CrossRef]

67. Lim, S.; Suh, K.; Kim, Y.; Yoon, M.; Park, H.; Dybtsev, D.N.; Kim, K. Porous carbon materials with a controllable surface area synthesized from metal-organic frameworks. *Chem. Commun.* **2012**, *48*, 7447–7449. [CrossRef]

68. Banerjee, A.; Upadhyay, K.K.; Puthusseri, D.; Aravindan, V.; Madhavi, S.; Ogale, S. MOF-derived crumpled-sheet-assembled perforated carbon cuboids as highly effective cathode active materials for ultra-high energy density Li-ion hybrid electrochemical capacitors (Li-HECs). *Nanoscale* **2014**, *6*, 4387. [CrossRef]

69. Chang, L.; Li, J.; Duan, X.; Liu, W. Porous carbon derived from Metal–organic framework (MOF) for capacitive deionization electrode. *Electrochim. Acta* **2015**, *176*, 956–964. [CrossRef]

70. Kukulka, W.; Cendrowski, K.; Michalkiewicz, B.; Mijowska, E. MOF-5 derived carbon as material for CO 2 absorption. *RSC Adv.* **2019**, *9*, 18527–18537. [CrossRef]

71. Segakweng, T.; Musyoka, N.M.; Ren, J.; Crouse, P.; Langmi, H.W. Comparison of MOF-5- and Cr-MOF-derived carbons for hydrogen storage application. *Res. Chem. Intermed.* **2016**, *42*, 4951–4961. [CrossRef]

72. Zou, G.; Jia, X.; Huang, Z.; Li, S.; Liao, H.; Hou, H.; Huang, L.; Ji, X. Cube-shaped Porous Carbon Derived from MOF-5 as Advanced Material for Sodium-Ion Batteries. *Electrochim. Acta* **2016**, *196*, 413–421. [CrossRef]

73. Park, K.S.; Ni, Z.; Côté, A.P.; Choi, J.Y.; Huang, R.; Uribe-Romo, F.J.; Chae, H.K.; O'Keeffe, M.; Yaghi, O.M. Exceptional chemical and thermal stability of zeolitic imidazolate frameworks. *Proc. Natl. Acad. Sci. USA* **2006**, *103*, 10186–10191. [CrossRef]

74. Jiao, L.; Jiang, H.-L. Metal-Organic-Framework-Based Single-Atom Catalysts for Energy Applications. *Chem* **2019**, *5*, 786–804. [CrossRef]

75. Zhu, Y.; Zhang, Z.; Li, W.; Lei, Z.; Cheng, N.; Tan, Y.; Mu, S.; Sun, X. Highly Exposed Active Sites of Defect-Enriched Derived MOFs for Enhanced Oxygen Reduction Reaction. *ACS Sustain. Chem. Eng.* **2019**, *7*, 17855–17862. [CrossRef]

76. Yang, S.L.; Zhu, Y.N.; Cao, C.Y.; Peng, L.; Li, S.M.; Zhai, D.W.; Song, W.G. A general route to coat poly(cyclotriphosphazene-co-4,4 '-sulfonyldiphenol) on various substrates and the derived N, P, S-doped hollow carbon shells for catalysis. *Nanoscale* **2017**, *9*, 13538–13545. [CrossRef]

77. Yang, S.L.; Peng, L.; Huang, P.P.; Wang, X.S.; Sun, Y.B.; Cao, C.Y.; Song, W.G. Nitrogen, Phosphorus, and Sulfur Co-Doped Hollow Carbon Shell as Superior Metal-Free Catalyst for Selective Oxidation of Aromatic Alkanes. *Angew. Chem. Int. Ed.* **2016**, *55*, 4016–4020. [CrossRef]

78. Liu, W.; Li, S.Q.; Liu, W.X.; Zhang, Q.; Shao, J.; Tian, J.L. MOF-derived B, N co-doped porous carbons as metal-free catalysts for highly efficient nitro aromatics reduction. *J. Environ. Chem. Eng.* **2021**, *9*, 105689. [CrossRef]

79. Wang, X.; Li, Y.W. Nanoporous carbons derived from MOFs as metal-free catalysts for selective aerobic oxidations. *J. Mater. Chem. A* **2016**, *4*, 5247–5257. [CrossRef]

80. Kim, B.R.; Oh, J.S.; Kim, J.; Lee, C.Y. Robust Aerobic Alcohol Oxidation Catalyst Derived from Metal-Organic Frameworks. *Catal. Lett.* **2016**, *146*, 734–743. [CrossRef]

81. Yao, X.F.; Bai, C.H.; Chen, J.Y.; Li, Y.W. Efficient and selective green oxidation of alcohols by MOF-derived magnetic nanoparticles as a recoverable catalyst. *RSC Adv.* **2016**, *6*, 26921–26928. [CrossRef]

82. Bhadra, B.N.; Jhung, S.H. Well-dispersed Ni or MnO nanoparticles on mesoporous carbons: Preparation via carbonization of bimetallic MOF-74s for highly reactive redox catalysts. *Nanoscale* **2018**, *10*, 15035–15047. [CrossRef] [PubMed]

83. Nguyen-Sorenson, A.H.T.; Anderson, C.M.; Balijepalli, S.K.; McDonald, K.A.; Matzger, A.J.; Stowers, K.J. Highly active copper catalyst obtained through rapid MOF decomposition. *Inorg. Chem. Front.* **2019**, *6*, 521–526. [CrossRef]

84. Murugesan, K.; Senthamarai, T.; Sohail, M.; Alshammari, A.S.; Pohl, M.M.; Beller, M.; Jagadeesh, R.V. Cobalt-based nanoparticles prepared from MOF-carbon templates as efficient hydrogenation catalysts. *Chem. Sci.* **2018**, *9*, 8553–8560. [CrossRef] [PubMed]

85. Niu, H.Y.; Liu, S.L.; Cai, Y.Q.; Wu, F.C.; Zhao, X.L. MOF derived porous carbon supported Cu/Cu2O composite as high performance non-noble catalyst. *Microporous Mesoporous Mater.* **2016**, *219*, 48–53. [CrossRef]

86. Rong, J.; Qiu, F.; Zhang, T.; Zhu, Y.; Xu, J.C.; Guo, Q.; Peng, X.M. Non-noble metal@carbon nanosheet derived from exfoliated MOF crystal as highly reactive and stable heterogeneous catalyst. *Appl. Surf. Sci.* **2018**, *447*, 222–234. [CrossRef]

87. Zhi, L.H.; Liu, H.; Xu, Y.Y.; Hu, D.C.; Yao, X.Q.; Liu, J.C. Pyrolysis of metal-organic framework (CuBTC) decorated filter paper as a low-cost and highly active catalyst for the reduction of 4-nitrophenol. *Dalton Trans.* **2018**, *47*, 15458–15464. [CrossRef]

88. Guo, X.L.; Chen, X.; Su, D.S.; Liang, C.H. Preparation of Ni/C Core-shell Nanoparticles through MOF Pyrolysis for Phenylacetylene Hydrogenation Reaction. *Acta Chim. Sin.* **2018**, *76*, 22–29. [CrossRef]

89. Nakatsuka, K.; Yoshii, T.; Kuwahara, Y.; Mori, K.; Yamashita, H. Controlled Pyrolysis of Ni-MOF-74 as a Promising Precursor for the Creation of Highly Active Ni Nanocatalysts in Size-Selective Hydrogenation. *Chem. Eur. J.* **2018**, *24*, 898–905. [CrossRef]

90. Zhang, L.L.; Chen, X.; Peng, Z.J.; Liang, C.H. Chemoselective hydrogenation of cinnamaldehyde over MOFs-derived M2Si@C (M = Fe, Co, Ni) silicides catalysts. *Mol. Catal.* **2018**, *449*, 14–24. [CrossRef]

91. Zhao, Y.J.; Wu, X.Q.; Zhou, J.H.; Wang, Y.; Wang, S.P.; Ma, X.B. MOF-derived Cu@C Catalyst for the Liquid-phase Hydrogenation of Esters. *Chem. Lett.* **2018**, *47*, 883–886. [CrossRef]

92. Dong, W.H.; Zhang, L.; Wang, C.H.; Feng, C.; Shang, N.Z.; Gao, S.T.; Wang, C. Palladium nanoparticles embedded in metal-organic framework derived porous carbon: Synthesis and application for efficient Suzuki-Miyaura coupling reactions. *RSC Adv.* **2016**, *6*, 37118–37123. [CrossRef]

93. Sun, W.; Gao, L.F; Sun, X.; Zheng, G.X. A novel route with a Cu(II)-MOF-derived structure to synthesize Cu/Cu2O NPs@graphene: The electron transfer leads to the synergistic effect of the Cu(0)-Cu(I) phase for an effective catalysis of the Sonogashira cross-coupling reactions. *Dalton Trans.* **2018**, *47*, 5538–5541. [CrossRef]

94. Cheng, S.S.; Shang, N.Z.; Feng, C.; Gao, S.T.; Wang, C.; Wang, Z. Efficient multicomponent synthesis of propargylamines catalyzed by copper nanoparticles supported on metal-organic framework derived nanoporous carbon. *Catal. Commun.* **2017**, *89*, 91–95. [CrossRef]

95. Dong, Z.P.; Le, X.D.; Liu, Y.S.; Dong, C.X.; Ma, J.T. Metal organic framework derived magnetic porous carbon composite supported gold and palladium nanoparticles as highly efficient and recyclable catalysts for reduction of 4-nitrophenol and hydrodechlorination of 4-chlorophenol. *J. Mater. Chem. A* **2014**, *2*, 18775–18785. [CrossRef]

96. Yamane, I.; Sato, K.; Otomo, R.; Yanase, T.; Miura, A.; Nagahama, T.; Kamiya, Y.; Shimada, T. Ultrahigh-Pressure Preparation and Catalytic Activity of MOF-Derived Cu Nanoparticles. *Nanomaterials* **2021**, *11*, 1040. [CrossRef]

97. Bai, C.H.; Li, A.Q.; Yao, X.F.; Liu, H.L.; Li, Y.W. Efficient and selective aerobic oxidation of alcohols catalysed by MOF-derived Co catalysts. *Green Chem.* **2016**, *18*, 1061–1069. [CrossRef]

98. Chen, H.R.; Shen, K.; Mao, Q.; Chen, J.Y.; Li, Y.W. Nanoreactor of MOF-Derived Yolk-Shell Co@C-N: Precisely Controllable Structure and Enhanced Catalytic Activity. *ACS Catal.* **2018**, *8*, 1417–1426. [CrossRef]

99. Ji, S.F.; Chen, Y.J.; Fu, Q.; Chen, Y.F.; Dong, J.C.; Chen, W.X.; Li, Z.; Wang, Y.; Gu, L.; He, W.; et al. Confined Pyrolysis within Metal-Organic Frameworks To Form Uniform Ru-3 Clusters for Efficient Oxidation of Alcohols. *J. Am. Chem. Soc.* **2017**, *139*, 9795–9798. [CrossRef]

100. Zhou, Y.; Long, J.L.; Li, Y.W. Ni-based catalysts derived from a metal-organic framework for selective oxidation of alkanes. *Chin. J. Catal.* **2016**, *37*, 955–962. [CrossRef]

101. Zhong, H.; Wang, Y.X.; Cui, C.Y.; Zhou, F.; Hu, S.Q.; Wang, R.H. Facile fabrication of Cu-based alloy nanoparticles encapsulated within hollow octahedral N-doped porous carbon for selective oxidation of hydrocarbons. *Chem. Sci.* **2018**, *9*, 8703–8710. [CrossRef]

102. Yu, G.L.; Sun, J.; Muhammad, F.; Wang, P.Y.; Zhu, G.S. Cobalt-based metal organic framework as precursor to achieve superior catalytic activity for aerobic epoxidation of styrene. *RSC Adv.* **2014**, *4*, 38804–38811. [CrossRef]

103. Hui, J.F.; Chu, H.M.; Zhang, W.L.; Shen, Y.; Chen, W.Z.; Hu, Y.; Liu, W.; Gao, C.; Guo, S.H.; Xiao, G.W.; et al. Multicomponent metal-organic framework derivatives for optimizing the selective catalytic performance of styrene epoxidation reaction. *Nanoscale* **2018**, *10*, 8772–8778. [CrossRef] [PubMed]

104. Zhou, Y.X.; Chen, Y.Z.; Cao, L.N.; Lu, J.L.; Jiang, H.L. Conversion of a metal-organic framework to N-doped porous carbon incorporating Co and CoO nanoparticles: Direct oxidation of alcohols to esters. *Chem. Commun.* **2015**, *51*, 8292–8295. [CrossRef] [PubMed]

105. Zhong, W.; Liu, H.L.; Bai, C.H.; Liao, S.J.; Li, Y.W. Base-Free Oxidation of Alcohols to Esters at Room Temperature and Atmospheric Conditions using Nanoscale Co-Based Catalysts. *ACS Catal.* **2015**, *5*, 1850–1856. [CrossRef]

106. Liu, X.M.; Cheng, S.J.; Long, J.L.; Zhang, W.; Liu, X.H.; Wei, D.P. MOFs-Derived Co@CN bi-functional catalysts for selective transfer hydrogenation of alpha,beta-unsaturated aldehydes without use of base additives. *Mater. Chem. Front.* **2017**, *1*, 2005–2012. [CrossRef]

107. Shen, K.; Chen, L.; Long, J.L.; Zhong, W.; Li, Y.W. MOFs-Templated Co@Pd Core Shell NPs Embedded in N-Doped Carbon Matrix with Superior Hydrogenation Activities. *ACS Catal.* **2015**, *5*, 5264–5271. [CrossRef]

108. Ma, X.; Zhou, Y.X.; Liu, H.; Li, Y.; Jiang, H.L. A MOF-derived Co-CoO@N-doped porous carbon for efficient tandem catalysis: Dehydrogenation of ammonia borane and hydrogenation of nitro compounds. *Chem. Commun.* **2016**, *52*, 7719–7722. [CrossRef]

109. Xu, X.J.; Li, H.; Xie, H.T.; Ma, Y.H.; Chen, T.X.; Wang, J.D. Zinc cobalt bimetallic nanoparticles embedded in porous nitrogen-doped carbon frameworks for the reduction of nitro compounds. *J. Mater. Res.* **2017**, *32*, 1777–1786. [CrossRef]

110. Jia, W.L.; Tian, F.P.; Zhang, M.J.; Li, X.Y.; Ye, S.; Ma, Y.F.; Wang, W.Y.; Zhang, Y.F.; Meng, C.G.; Zeng, G.; et al. Nitrogen-doped porous carbon-encapsulated copper composite for efficient reduction of 4-nitrophenol. *J. Colloid Interface Sci.* **2021**, *594*, 254–264. [CrossRef]

111. Sun, X.; Olivos-Suarez, A.I.; Oar-Arteta, L.; Rozhko, E.; Osadchii, D.; Bavykina, A.; Kapteijn, F.; Gascon, J. Metal-Organic Framework Mediated Cobalt/Nitrogen-Doped Carbon Hybrids as Efficient and Chemoselective Catalysts for the Hydrogenation of Nitroarenes. *ChemCatChem* **2017**, *9*, 1854–1862. [CrossRef]

112. Liu, K.J.; Luo, K.J.; Tan, H.; Li, N.; Hu, B.N.; Ou, J.H. Preparation of Co-based N-doped Meso-microporous Carbon for Hydrogenation of Nitroarenes. *ChemistrySelect* **2022**, *7*, e202202288. [CrossRef]

113. Chen, Y.Z.; Cai, G.R.; Wang, Y.M.; Xu, Q.; Yu, S.H.; Jiang, H.L. Palladium nanoparticles stabilized with N-doped porous carbons derived from metal-organic frameworks for selective catalysis in biofuel upgrade: The role of catalyst wettability. *Green Chem.* **2016**, *18*, 1212–1217. [CrossRef]

114. Long, J.L.; Zhou, Y.; Li, Y.W. Transfer hydrogenation of unsaturated bonds in the absence of base additives catalyzed by a cobalt-based heterogeneous catalyst. *Chem. Commun.* **2015**, *51*, 2331–2334. [CrossRef]

115. Long, J.L.; Shen, K.; Chen, L.; Li, Y.W. Multimetal-MOF-derived transition metal alloy NPs embedded in an N-doped carbon matrix: Highly active catalysts for hydrogenation reactions. *J. Mater. Chem. A* **2016**, *4*, 10254–10262. [CrossRef]

116. Bennedsen, N.R.; Kramer, S.; Mielby, J.J.; Kegnaes, S. Cobalt-nickel alloy catalysts for hydrosilylation of ketones synthesized by utilizing metal-organic framework as template. *Catal. Sci. Technol.* **2018**, *8*, 2434–2440. [CrossRef]

117. Li, X.L.; Zhang, W.; Liu, Y.S.; Li, R. Palladium Nanoparticles Immobilized on Magnetic Porous Carbon Derived from ZIF-67 as Efficient Catalysts for the Semihydrogenation of Phenylacetylene under Extremely Mild Conditions. *ChemCatChem* **2016**, *8*, 1111–1118. [CrossRef]

118. Ding, S.S.; Zhang, C.H.; Liu, Y.F.; Jiang, H.; Chen, R.Z. Selective hydrogenation of phenol to cyclohexanone in water over Pd@N-doped carbons derived from ZIF-67: Role of dicyandiamide. *Appl. Surf. Sci.* **2017**, *425*, 484–491. [CrossRef]

119. Ding, S.S.; Zhang, C.H.; Liu, Y.F.; Jiang, H.; Xing, W.H.; Chen, R.Z. Pd nanoparticles supported on N-doped porous carbons derived from ZIF-67: Enhanced catalytic performance in phenol hydrogenation. *J. Ind. Eng. Chem.* **2017**, *46*, 258–265. [CrossRef]

120. Jagadeesh, R.V.; Murugesan, K.; Alshammari, A.S.; Neumann, H.; Pohl, M.M.; Radnik, J.; Beller, M. MOF-derived cobalt nanoparticles catalyze a general synthesis of amines. *Science* **2017**, *358*, 326–332. [CrossRef]

121. Wang, X.; Chen, W.X.; Zhang, L.; Yao, T.; Liu, W.; Lin, Y.; Ju, H.X.; Dong, J.C.; Zheng, L.R.; Yan, W.S.; et al. Uncoordinated Amine Groups of Metal-Organic Frameworks to Anchor Single Ru Sites as Chemoselective Catalysts toward the Hydrogenation of Quinoline. *J. Am. Chem. Soc.* **2017**, *139*, 9419–9422. [CrossRef]

122. Zhang, L.; Feng, C.; Gao, S.T.; Wang, Z.; Wang, C. Palladium nanoparticle supported on metal-organic framework derived N-decorated nanoporous carbon as an efficient catalyst for the Suzuki coupling reaction. *Catal. Commun.* **2015**, *61*, 21–25. [CrossRef]

123. Bugday, N.; Altin, S.; Yasar, S. Palladium nanoparticle supported on nitrogen-doped porous carbon: Investigation of structural properties and catalytic activity on Suzuki-Miyaura reactions. *Appl. Organomet. Chem.* **2021**, *35*, e6403. [CrossRef]

124. Ning, X.; Sun, Y.H.; Fu, H.Y.; Qu, X.L.; Xu, Z.Y.; Zheng, S.R. N-doped porous carbon supported Ni catalysts derived from modified Ni-MOF-74 for highly effective and selective catalytic hydrodechlorination of 1,2-dichloroethane to ethylene. *Chemosphere* **2020**, *241*, 124978. [CrossRef] [PubMed]

125. Cui, X.L.; Zuo, W.; Tian, M.; Dong, Z.P.; Ma, J.T. Highly efficient and recyclable Ni MOF-derived N-doped magnetic mesoporous carbon-supported palladium catalysts for the hydrodechlorination of chlorophenols. *J. Mol. Catal. A Chem.* **2016**, *423*, 386–392. [CrossRef]

126. Toyao, T.; Fujiwaki, M.; Miyahara, K.; Kim, T.H.; Horiuchi, Y.; Matsuoka, M. Design of Zeolitic Imidazolate Framework Derived Nitrogen-Doped Nanoporous Carbons Containing Metal Species for Carbon Dioxide Fixation Reactions. *ChemSusChem* **2015**, *8*, 3905–3912. [CrossRef]

127. Ding, M.L.; Chen, S.; Liu, X.Q.; Sun, L.B.; Lu, J.L.; Jiang, H.L. Metal-Organic Framework-Templated Catalyst: Synergy in Multiple Sites for Catalytic CO2 Fixation. *ChemSusChem* **2017**, *10*, 1898–1903. [CrossRef]

128. Chen, F.F.; Shen, K.; Chen, L.Y.; Li, Y.W. N-doped nanocarbon embedded in hierarchically porous metal-organic frameworks for highly efficient CO2 fixation. *Sci. China-Chem.* **2022**, *65*, 1411–1419. [CrossRef]

129. Wang, Z.Z.; Zhou, X.H.; Gong, S.F.; Xie, J.W. MOF-Derived Cu@N-C Catalyst for 1,3-Dipolar Cycloaddition Reaction. *Nanomaterials* **2022**, *12*, 1070. [CrossRef]

130. Li, X.L.; Zhang, B.Y.; Fang, Y.H.; Sun, W.J.; Qi, Z.Y.; Pei, Y.C.; Qi, S.Y.; Yuan, P.Y.; Luan, X.C.; Goh, T.W.; et al. Metal-Organic-Framework-Derived Carbons: Applications as Solid-Base Catalyst and Support for Pd Nanoparticles in Tandem Catalysis. *Chem. Eur. J.* **2017**, *23*, 4266–4270. [CrossRef]

131. Xie, F.; Chen, Q.H.; Xie, R.; Jiang, H.F.; Zhang, M. MOF-Derived Nanocobalt for Oxidative Functionalization of Cyclic Amines to Quinazolinones with 2-Aminoarylmethanols. *ACS Catal.* **2018**, *8*, 5869–5874. [CrossRef]

132. Zhao, X.; Fang, R.; Wang, F.; Kong, X.; Li, Y. Atomic design of dual-metal hetero-single-atoms for high-efficiency synthesis of natural flavones. *Nat. Commun.* **2022**, *13*, 10. [CrossRef] [PubMed]

133. Long, J.L.; Shen, K.; Li, Y.W. Bifunctional N-Doped Co@C Catalysts for Base-Free Transfer Hydrogenations of Nitriles: Controllable Selectivity to Primary Amines vs Imines. *ACS Catal.* **2017**, *7*, 275–284. [CrossRef]

134. Pérez-Mayoral, E.; Calvino-Casilda, V.; Soriano, E. Metal-supported carbon-based materials: Opportunities and challenges in the synthesis of valuable products. *Catal. Technol.* **2016**, *6*, 1265–1286. [CrossRef]

135. Pérez-Mayoral, E.; Lopez-Peinado, A.J. Porous Catalytic Systems in the Synthesis of Bioactive Heterocycles and Related Compound. In *Green Synthetic Approaches for Biologically Relevant Heterocycles*, 2nd ed.; Brahmachari, G., Ed.; Volume 2: Green Catalytic Systems and Solvents; Elsevier: Amsterdam, The Netherlands, 2021; pp. 97–164.

136. Wang, C.; Kim, J.; Tang, J.; Kim, M.; Lim, H.; Malgras, V.; You, J.; Xu, Q.; Li, J.; Yamauchi, Y. New strategies for novel MOF-derived carbon materials based on nanoarchitectures. *Chem* **2020**, *6*, 19–40. [CrossRef]